Karst of the Driftless Area of Jo Daviess County, Illinois

Samuel V. Panno,[1] Donald E. Luman,[1] Walton R. Kelly,[2]
Timothy H. Larson,[1] and Steven J. Taylor[3]

[1]Illinois State Geological Survey, [2]Illinois State Water Survey, and [3]Illinois Natural History Survey,
Prairie Research Institute, University of Illinois at Urbana-Champaign

Circular 586 2017

ILLINOIS STATE
GEOLOGICAL SURVEY
PRAIRIE RESEARCH INSTITUTE

ILLINOIS STATE GEOLOGICAL SURVEY
Prairie Research Institute
University of Illinois at Urbana-Champaign

Front cover: *Crevice caves, and crevices and fractures are commonly seen in quarries that expose vertical surfaces of carbonate rock. Bedding planes are also visible, and many are solution-enlarged, allowing for groundwater movement. Photograph by Samuel V. Panno; used by permission.*

Karst of the Driftless Area of Jo Daviess County, Illinois

Samuel V. Panno,[1] Donald E. Luman,[1] Walton R. Kelly,[2]
Timothy H. Larson,[1] and Steven J. Taylor[3]

[1]Illinois State Geological Survey, [2]Illinois State Water Survey, and [3]Illinois Natural History Survey,
Prairie Research Institute, University of Illinois at Urbana-Champaign

Circular 586 2017

ILLINOIS STATE GEOLOGICAL SURVEY
PRAIRIE RESEARCH INSTITUTE

ILLINOIS

ILLINOIS STATE GEOLOGICAL SURVEY
Prairie Research Institute
University of Illinois at Urbana-Champaign
615 E. Peabody Drive
Champaign, Illinois 61820-6918
http://www.isgs.illinois.edu

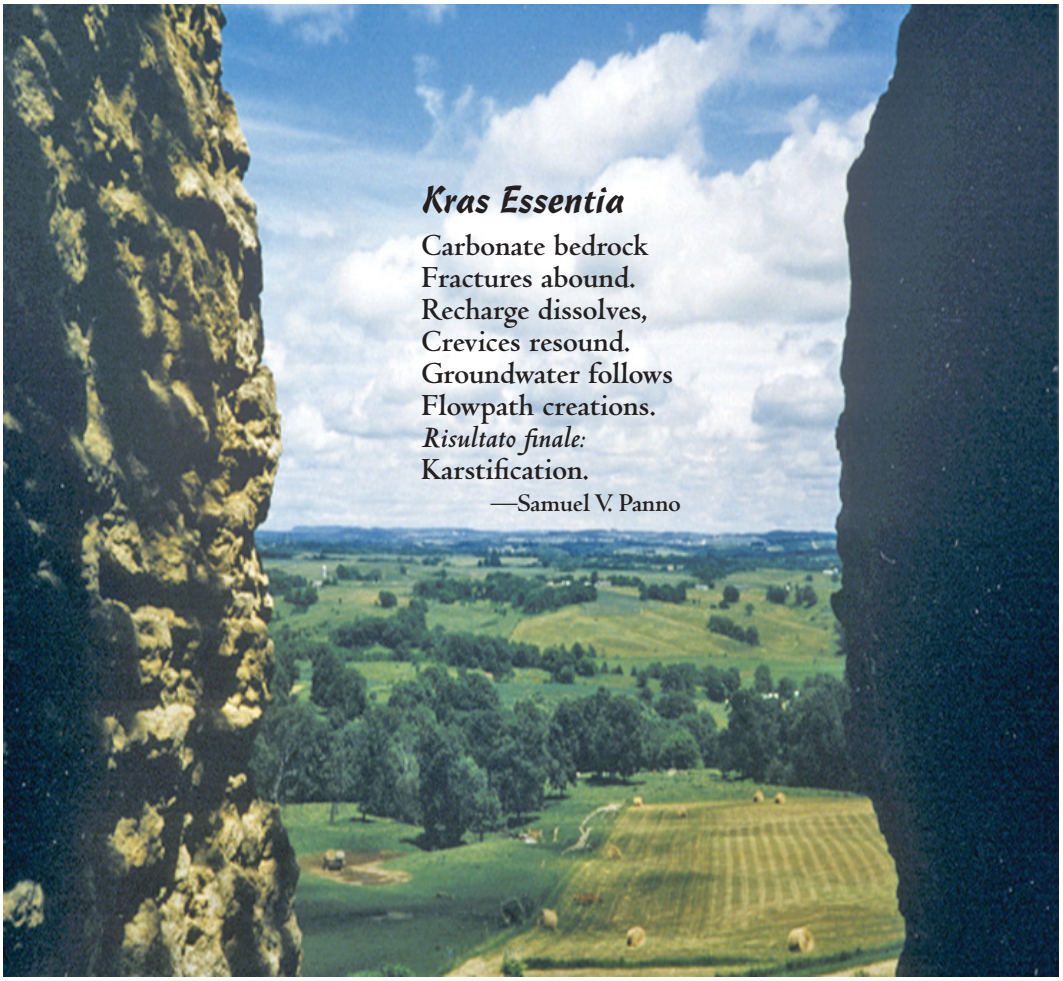

Suggested citation:
Panno, S.V., D.E. Luman, W.R. Kelly, T.H. Larson, and S.J. Taylor, 2017, Karst of the Driftless Area of Jo Daviess County, Illinois: Illinois State Geological Survey, Circular 586, 39 p.

CONTENTS

Abstract 1

Introduction 1
- Geology 1
- Karst Defined 2

Methodology 4
- Aerial Photography 4
- Lidar Elevation Data 4
- Ground-Penetrating Radar 4
- Field Observations 4
- Groundwater Chemistry 4

Results and Discussion 5
- Geology and Hydrogeology of Jo Daviess County 5
- Vegetated Crop Lines 7
- Lidar Elevation Models 10
  - Silurian Dolomite 10
  - Ordovician Galena Dolomite 13
- Ground-Penetrating Radar 13
- Bedrock Exposures in Road Cuts and Quarries 15
  - Savanna Blacktop and Quarry 15
  - Illinois Route 78 Road Cut (near the Wisconsin Border) 18
  - U.S. Route 20 Road Cuts 18
  - Louis' Aggregate Stockton Quarry 20
  - Civil Quarry 23
  - Crawford Quarry 23
  - Good Miller Quarry 23
  - Miner Road Quarry 24
- Recharge to and Groundwater Flow Within the Galena Dolomite 24
- Hydrologic Features 25
  - Springs 25
  - Chemical Composition of Groundwater 25

Summary and Conclusions 36

Acknowledgments 36

References 36

Tables
1. Range of concentrations and estimated background threshold values for parameters and ions determined from spring-water samples collected by Maas (2010) in eastern Jo Daviess County 28
2. Groundwater samples collected from 11 shallow wells and one spring from across Jo Daviess County in July 2014 30

Figures
1. Source areas for glacial ice on the North American continent during the Pleistocene Epoch 1
2. Stratigraphy of Ordovician and Silurian bedrock in Jo Daviess County 3
3. Map of the karst regions of Illinois 3
4. Generalized geologic map of Jo Daviess County 6
5. Cross section of northwestern Illinois showing dipping beds associated with the Wisconsin Arch and bedrock exposures 6
6. Structural features surrounding Jo Daviess County 7
7. Map of the Upper Mississippi Valley Zinc-Lead District within Jo Daviess County 8
8. Solution-enlarged crevices are common karst features in northwestern Illinois and are exposed in road cuts, quarries, and outcrops 10

9 Crop lines in an alfalfa field in eastern Jo Daviess County during July 2012 as seen (a) from the ground and (b) oblique from the air. (c) Crop lines in an alfalfa field in eastern Jo Daviess County in August 2012 as seen from Google aerial photography 10
10 (a) Cover-collapse sinkholes in unconsolidated sediment overlying creviced Silurian dolomite in a contoured lidar elevation model (contour interval = 5 ft [1.5 m]). (b) A 3-ft (1-m)-wide crevice in Silurian dolomite, oriented in an east–west direction and located in a road cut across from the Long Hollow Scenic Overlook located between Galena and Elizabeth, Illinois 11
11 Cover-collapse sinkholes in unconsolidated sediment overlying creviced Silurian dolomite 11
12 A 3-ft (1-m)-diameter conduit within Silurian dolomite showing the development of frost as a result of warm, moist air discharging from the entrance 12
13 Mining scars in Galena Dolomite from the Vinegar Hills Mine area just north of Galena, Illinois, as seen in a lidar bare-earth elevation model showing linear excavations from zinc–lead mining that appear as east–west-trending holes 12
14 A tilted block of Silurian dolomite along a highland slowly sliding downhill on Maquoketa Shale 13
15 Spring within the Hanover Bluff Nature Preserve discharging from an 0.8-in. (2-cm)-wide crevice near the base of the Silurian dolomite 13
16 Photomosaic of a road cut located just east of Elizabeth, Illinois, along U.S. Route 20, Jo Daviess County (looking south), showing solution-enlarged crevices in the Galena Dolomite 14
17 Photomosaic of a road cut (both sides of the road) located on Illinois Route 78 just southeast of the Wisconsin border (Map 1), showing abundant solution-enlarged crevices in the Galena Dolomite 16
18 (a) Cave within Galena Dolomite just east of Elizabeth, Illinois. (b) Cover-collapse sinkhole in unconsolidated material overlying Galena Dolomite in eastern Jo Daviess County 16
19 A karst spring discharging from a crevice at the base of the tree within the Galena Dolomite and draining off to a nearby stream 17
20 Angular stream channel (see arrow) as revealed on a lidar bare-earth elevation model showing bedrock-controlled, angular stream geometry within the Galena Dolomite 17
21 Ground-penetrating radar (GPR) locations of and data on crevices within the Galena Dolomite exposed within a road cut along Illinois Route 78 just south of Warren, Illinois (Map 1) 18
22 Ground-penetrating radar (GPR) location and data, and an aerial photograph of a field located just south of Warren, Illinois (Map 1), showing multiple fractures and crevices within a field 19
23 Working face of the Savanna Blacktop and Quarry located just south of the Jo Daviess County border in Carroll County 20
24 Detail of a fault zone on the southwestern side of the Illinois Route 78 road cut (Map 1) showing a displacement of about 6 ft (2 m) 21
25 Detail of a fault zone on the northwest side of the Illinois Route 78 road cut (Map 1) showing a displacement of about 6 in. (15 cm) 21
26 Alignment of crop lines (left) with crevices in a road cut (right; Map 1) 21
27 Detail of a collapse zone on the northeastern side of the Illinois Route 78 road cut (Map 1) 22
28 (a) Crevice trending east–west in a wall of the Louis' Aggregate Stockton Quarry (Map 1). (b) Crevice trending north–south and filled with fine-grained sediment within the Louis' Aggregate Stockton Quarry with a gob pile in the foreground 23
29 Blast damage in a working face at the Louis' Aggregate Stockton Quarry (Map 1) 23
30 Three east–west-oriented crevices in the working face of Civil Quarry (Map 1) 24
31 Aerial photograph of the Crawford Quarry (Map 1) showing a fracture–crevice pattern in the quarry floor that is enhanced by vegetation 24
32 Numerous crevices oriented roughly east–west and ranging from tight fractures to more than 1 ft (30 cm) wide are common in the Good Miller Quarry located just south of Stockton, Illinois (Map 1) 25
33 Crevice caves (a) and crevices and fractures (a, b) are common within the Galena Dolomite at the Miner Road Quarry (Map 1) 25
34 Springs within the Galena Dolomite in Jo Daviess County discharge at rates of <1 to 10 L/s (Map 1) 26

35 Spring temperature versus time showing the variability of seasonal spring-water temperatures 27
36 Cl^- (mg/L) versus depth (ft) in the Galena and Platteville Groups for municipal wells in Jo Daviess County 29
37 NO_3-N (mg/L) versus depth (ft) in the Galena and Platteville Groups for municipal wells in Jo Daviess County showing the greatest enrichment in the upper 150 ft (46 m) 29
38 Ca plus Mg versus HCO_3^- (mmol/L) showing the effects of dissolution of dolomite, potentially mixed with the effects of the oxidation of pyrite 29
39 K versus Cl^- (mg/L) showing spring-water samples relative to background concentrations of each ion 32
40 NO_3-N (mg/L) versus time showing the effects of surface-borne contamination on the six springs 32
41 Cl^- versus NO_3-N (mg/L) for spring-water samples 33
42 Na versus Cl^- (mg/L) showing a strong correlation between the two ions 33
43 NO_3-N (mg/L) versus tritium (TU) showing an increase in NO_3-N concentrations with an increase in tritium concentrations 34
44 F^- (mg/L) and tritium (TU) covary, albeit with limited data, suggesting that F^- increases in concentration with time within the karst aquifer, probably because of rock–water interaction 34
45 SO_4^{2-} versus Ca (mg/L) in shallow wells reveals a linear relationship that is common in groundwater 35
46 δD versus $\delta^{18}O$ for precipitation in Chicago, Illinois (Chicago Midway International Airport), from January 1960 through December 1979, and 12 tightly clustered groundwater samples collected from Jo Daviess County 35

ABSTRACT

Karst aquifers are vulnerable to groundwater contamination because of their unique characteristics of rapid recharge via sinkholes, thin soils, or both, as well as their rapid groundwater flow velocities through fractures, solution-enlarged crevices, and conduits. Information on the identification and characterization of karst regions is thus critical when making land-use decisions so that groundwater resources in Illinois are sufficiently protected.

This investigation was conducted in Jo Daviess County and had two aspects: (1) an investigation of the karst features present in the carbonate bedrock of the Ordovician Galena Dolomite, Silurian dolomite, and overlying sediments, and (2) and an assessment of groundwater quality within aquifers of the Galena and Platteville Groups. Our investigation revealed abundant evidence of karstified carbonate rock and the presence of karst aquifers throughout Jo Daviess County. Karst features in both Silurian and Ordovician carbonate rocks are dominated by solution-enlarged crevices 0.4 in. (1 cm) to 3 ft (1 m) wide within most road cuts and quarries examined throughout the county. Other karst features include cover-collapse sinkholes ranging from 3 to 25 ft (1 to 8 m) in diameter overlying the Galena Dolomite, cover-collapse sinkholes ranging from 60 to 100 ft (20 to 30 m) in diameter overlying the Silurian dolomite, and karst springs, caves, conduits, and solution-enlarged bedding planes in both formations. Recently, vegetated crop lines that developed during the drought of 2012 throughout Jo Daviess County and adjacent areas of the Driftless Area were revealed by aerial photography (Panno et al. 2015). Vegetated crop lines provided a much more detailed and complete expression of the complexity of fractures and solution-enlarged crevices of the underlying Galena Dolomite and reflected the fabric of the underlying karst aquifer. Road cuts and quarries provided information regarding the character and apertures of fractures and crevices at depth. Specifically, the exposures show that most crevices are filled with fine-grained sediment that, unless penetrated by tree roots, for example, can slow recharge. However, the smaller, more abundant aperture fractures are less likely to be filled by sediment and can provide pathways for rapid recharge to the underlying aquifer. In addition, crevices and conduits tend to be unfilled at depths near and below 50 ft (15 m), presumably providing pathways for rapid groundwater flow.

The aerial and vertical distributions of chloride and nitrate concentrations within the aquifer (from records and sampling of domestic wells) indicated rapid recharge and an open aquifer system consistent with a karst aquifer. Analysis of groundwater samples from 10 shallow wells open to the Galena Dolomite from across Jo Daviess County revealed stratification of surface-borne contaminants that extended to depths of 210 ft (64 m). These data suggest the aquifer is an open system that is not in equilibrium with dolomite, and they support previous interpretations that the Galena Dolomite constitutes a prolific karst aquifer within Jo Daviess County and the surrounding areas.

INTRODUCTION

Geology

Jo Daviess County in northwestern Illinois represents the southernmost extent of the Driftless Area, which includes southwestern Wisconsin, southeastern Minnesota, and northeastern Iowa. The Driftless Area is so named because it escaped the direct effects of Pleistocene glaciation. The area is described by B. Brandon Curry (ISGS, personal communication, August 2015) as follows: "bedrock-defended uplands gently dissected by wide-valleyed tributaries of the Mississippi River. Along the Mississippi River valley and lower reaches of the tributaries are patches of glaciofluvial deposits that show, even though the Driftless Area was never covered by ice; glacially related deposits (loess, outwash) are common throughout the county." In *Mysteries of the Driftless: The Documentary* (Nelson and Bertalan 2013), the late Jim Knox (University of Wisconsin) explained the reason the Driftless Area remained driftless during the Pleistocene Epoch. Knox stated that the lack of glaciation in the Driftless Area resulted from a combination of three factors: (1) resistance or friction from the Wisconsin Arch (Precambrian granitic rocks bowed up from Chicago to northern Wisconsin) at the base of each ice flow; (2) a diversion of Keewatin-centered glacial ice to the west by the Lake Superior Syncline that diverted ice into Minnesota; and (3) a diversion of Labrador-centered glacial ice by the Paleozoic shale bedrock to the east that was deeply eroded, channeling the ice to the southeast along these "slippery" rocks. Knox pointed out that at no time was the Driftless Area *surrounded* by glacial ice (Figure 1).

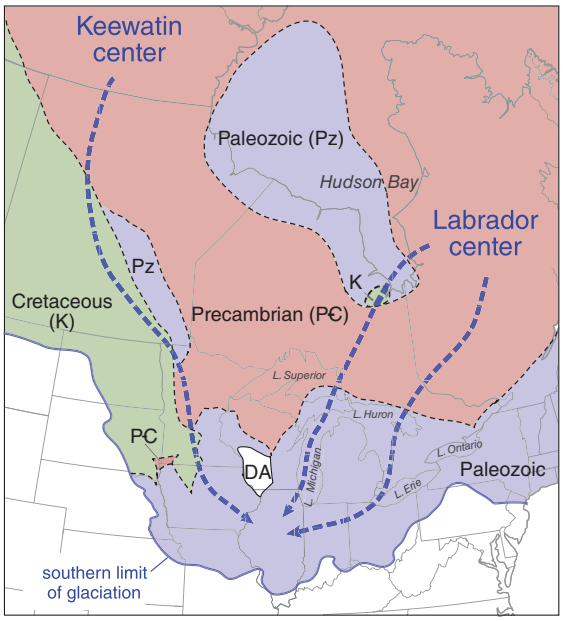

Figure 1 Source areas for glacial ice on the North American continent during the Pleistocene Epoch (from Hansel and McKay 2010). These include the Keewatin and Labrador centers in Canada, where snow and ice accumulated and spread out as ice sheets as far south as southern Illinois. DA, Driftless Area.

Bedrock within Jo Daviess County is dominated by Ordovician and Silurian carbonate rock. The Upper Ordovician strata consists of dolomite and lesser amounts of limestone of the Galena Group (also referred to as the "Galena Dolomite") and the Platteville Group. These are overlain by the Maquoketa Shale Group (hereafter referred to as the "Maquoketa Shale") and dolomite of the Silurian System (also referred to as the "Silurian dolomite") in the highlands. The fractured and creviced carbonate rocks of the Galena and Platteville Groups (Figure 2) constitute the aquifer used extensively by private individuals and municipalities. Bedrock in Jo Daviess County is overlain by a relatively thin layer of unconsolidated material (residuum and loess) that ranges from near zero to approximately 24.6 ft (7.5 m; Piskin and Bergstrom 1975).

Carbonate rock constitutes approximately 25% of the bedrock surface of Illinois (Weibel and Panno 1997) and ranges from Ordovician to Mississippian in age. Glacial drift and loess overlying carbonate bedrock range from 0 to >305 ft (0 to >100 m) and are thinnest in the Driftless Areas of northwestern Illinois and far southern Illinois. Carbonate bedrock is exposed at or closest to the surface along the margins of the Illinois Basin and along major structural features such as the La Salle Anticlinorium. In areas where carbonate rock is located at or near the surface (overlain by 0 to <50 ft [0 to <15 m] of unconsolidated sediment), karst features may be present at the surface (Figure 3).

Aquifers in carbonate rock are major sources of groundwater in Illinois and throughout the world. The most productive aquifers have secondary porosity (e.g., fractures, solution-enlarged crevices, conduits, and bedding plane partings), which permits the transport of much more water into and through the rock than does primary porosity. Carbon dioxide (CO_2) generated by root respiration and microbial activity in soils overlying carbonate rock causes infiltrating water (slightly acidic rainwater and snowmelt) to become more acidic before entering fractures, joints, and bedding planes in carbonate rock. The interaction of CO_2-charged soil water and groundwater with the carbonate bedrock causes small amounts of calcite, dolomite, or both (the dominant minerals in carbonate rock) to dissolve, releasing calcium (Ca), magnesium (Mg), and bicarbonate ions into groundwater at increasingly higher concentrations until the water approaches saturation with these minerals (White 1988). Slow dissolution of these rocks over thousands to hundreds of thousands of years gradually enlarges joints, fractures, and pathways along the bedding planes through which groundwater moves. Some solution-enlarged pathways become relatively large conduits through which groundwater flows rapidly from points of recharge (e.g., fractures) to points of discharge (e.g., springs). Consequently, the inherent solubility of carbonate rock is responsible for the development of karst.

Karst Defined

More than 25% of the world's population either lives on or obtains its water from karst aquifers. In the United States, 20% of the land surface is karst and 40% of the groundwater used for drinking comes from karst aquifers (Karst Water Institute 2014). The late James Quinlan, a leading expert in karst hydrogeology, stated that if the bedrock of an area is composed of carbonate rock, the area should be considered karst and assumed to be underlain by a karst aquifer unless proven otherwise. Of those areas within Illinois that are underlain by carbonate rock, 35% (9% of the state) are located in five regions that contain karst features at or near the surface (Panno et al. 1997; Weibel and Panno 1997; Panno and Weibel 2010; Figure 3). However, areas with karst aquifers do not necessarily display karst features at the surface. E. Calvin Alexander Jr., hydrogeologist and karst expert from the University of Minnesota, stated that the apparent absence of karst features on the ground surface (e.g., sinkholes) in no way precludes the presence of an underlying karst aquifer. This is because sinkholes, often considered the hallmark of karst, are end members of a continuum that extends from large-scale sinkhole drains down to nanoscale desiccation cracks (E.C. Alexander, personal communication, 2009). All these features may provide unrestricted flow from the surface to the subsurface and underlying aquifer.

We have reviewed the literature on the geology, geomorphology, and hydrogeology of karst and its various definitions (Quinlan 1966; Jennings 1971; White 1988; Ford and Williams 1989; Klimchouk and Ford 2000; Schilling and Helmers 2008a,b; Lindsey et al. 2010) and, on that basis, have developed the following working definition of karst for Illinois:

> *Karst (n.) is a geologically and hydrologically integrated or interconnected and self-organizing network of landforms and subsurface large-scale, secondary porosity created by a combination of fractured carbonate bedrock, the movement of water into and through the rock body as part of the hydrologic cycle, and physical and chemical weathering.*

Thus, karst refers to both a surface and subsurface landscape formed by the interaction of relatively aggressive surface water and shallow groundwater with soluble bedrock (i.e., limestone, dolomite, or both). The result is the formation of an ever-growing system of connected porosity (fractures, crevices, conduits) through which groundwater can, under a normal range of hydraulic gradients, flow more rapidly than in any other aquifer type. Groundwater flow rates can be feet to miles per hour instead of inches to feet per year, as is typical of other types of aquifers. This fracture–crevice–conduit system is responsible for the relatively high permeability and self-organizing qualities of the carbonate rock aquifers of Illinois. A "karst aquifer" is formed when the fractures of the rock are widened to about 0.4 in. (1 cm) or greater, allowing rapid and at times turbulent groundwater flow within the aquifer (White 1988). In areas with sinkholes and thin soils, the hydraulic connection between precipitation and aquifer recharge can be immediate. Because of the preferential fracture orientation, groundwater flow can be directional, leading to enhanced dissolution and crevice or conduit development. Consequently, the susceptibility of such an aquifer to the infiltration

SYSTEM	SERIES	GROUP	FORMATION Thickness (ft)	LITHOLOGY	DESCRIPTION
SILURIAN	NIAGARAN		Racine 300		Dolomite, pure, gray, thin-bedded to massive; local areas of brownish gray, argillaceous dolomite.
			Marcus 35–45		Dolomite, very pure, buff, vesicular, massive; contains *Pentamerus* in great abundance in lower 5–15 ft.
	ALEXANDRIAN		Sweeney 45–55		Dolomite, pure, pinkish gray; in thin wavy beds with green shale partings; corals abundant; 3–5 ft cherty zone near middle contains *Microcardinalia* and *Pentamerus*.
			Blanding 25–35		Dolomite, pure, brownish gray; contains many layers of white chert; silicified corals abundant; lower 3–5 ft slightly argillaceous.
			Tete des Morts 15–20		Dolomite, light gray, slightly cherty, thick-bedded medium to fine-grained, relatively pure.
			Mosalem 0–100		Dolomite, gray, cherty, medium-bedded; lower part is very argillaceous dolomite grading to dolomitic shale at base.
ORDOVICIAN	CINCINNATIAN	Maquoketa	Brainard 0–50		Shale, greenish gray, dolomitic; interbedded with fine- to medium-grained, argillaceous dolomite; abundant and diverse fauna consisting largely of brachiopods and bryozoans.
			Fort Atkinson 0–10		Dolomite, yellowish gray, fine-grained, argillaceous, thin-bedded; interbedded with greenish gray shale.
			Scales 125		Shale, gray, dolomitic; conchoidal fractures; *Isotelus* common in upper part; dark brown, carbonaceous, laminated shale in lower 15 ft; one or two beds of brown argillaceous dolomite at base containing depauperate fauna, pyrite, and phosphatic pebbles.
ORDOVICIAN	CHAMPLAINIAN	Galena	Dubuque 30–45		Dolomite, argillaceous, light gray to buff, fine- to medium-grained, thin- to medium-bedded; brown shale partings.
			Wise Lake 70–80		Dolomite, pure, light gray to buff, medium-grained, thick-bedded to massive; abundant molluscan fauna; *Receptaculites* abundant near middle
			Dunleith 130		Dolomite, gray to buff, medium-grained, thin- to thick-bedded; white to dark gray chalky and vitreous chert, particularly in upper part; *Receptaculites* abundant. Lower part argillaceous, sandy, fossiliferous, with green shale partings.
			Guttenberg 2–15		Dolomite and limestone, argillaceous, gray to brown, fine- to medium-grained, thin-bedded; reddish brown shale partings; abundant and diverse fauna.
		Platteville	Quimbys Mill 12		Dolomite, slightly argillaceous, light gray to buff, fine-grained, thin- to medium-bedded.
			Nachusa 20		Dolomite, pure, light gray to buff, thick-bedded, medium-grained, vuggy, fucoidal; white to light gray chert.
			Grand Detour 15–45		Dolomite and limestone, light gray to buff, thin- to medium-bedded, fine-grained; reddish brown shale partings; fossiliferous.
			Mifflin 15–25		Dolomite and limestone, argillaceous, light gray to buff, thin-bedded, fine-grained; greenish gray to blue-gray shale partings; fossiliferous.
			Pecatonica 20–30		Dolomite and limestone, light gray to buff, thin- to medium-bedded, fine-grained; brownish gray shale partings; corrosion surface at top; well-rounded sand grains in lower part.
		Ancell	Glenwood 5–20		Shale, sandstone, and dolomite, greenish gray; poorly sorted, fine- to coarse-grained sand.
			St. Peter 50–200		Sandstone, white, fine-grained, well-rounded, well-sorted, friable, thick-bedded to massive.

Figure 2 Stratigraphy of Ordovician and Silurian bedrock in Jo Daviess County (from Frankie and Nelson 2002).

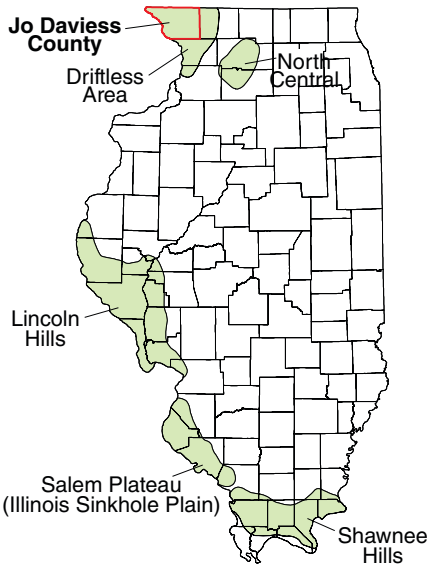

Figure 3 Map of the karst regions of Illinois (from Panno et al. 2014, 2016; modified from Weibel and Panno 1997). Note Jo Daviess County in the upper left-hand corner of the state.

of surface-borne contaminants can be high and groundwater quality can be adversely affected.

Knowing where karst areas are located and the degree of karstification present is important for land-use planning and water-resource considerations. As stated previously, recharge can be rapid, with little or no attenuation of surface-borne contaminants (filtering or chemical and microbial degradation) before they enter a karst aquifer, and groundwater flow velocities may be quite high. Consequently, it is important to thoroughly characterize the geology and hydrogeology of areas underlain by carbonate rock to identify and assess karst for water-resource protection and regulatory purposes. The objective of this investigation was to further characterize the surficial and bedrock geology and hydrogeology of the Driftless Area in Jo Daviess County. The research described herein expands on the work conducted by Weibel and Panno (1997), Panno et al. (1997, 2014, 2015), Panno and Luman (2008), and McGarry and Riggs (2000).

METHODOLOGY

The study area consisted of all of Jo Daviess County. Various methodologies were used to investigate the geology and hydrogeology of the county, including analysis and interpretation of historic and recently acquired aerial photography, recently acquired light detection and ranging (lidar) elevation data, ground-penetrating radar (GPR) of selected areas, field observations, and groundwater chemistry of springs and private wells.

Aerial Photography

As part of its National Agriculture Inventory Program (NAIP), the U.S. Department of Agriculture's Farm Service Agency acquires statewide digital orthophotography annually during the summer season. The NAIP imagery acquired for Jo Daviess County on June 27, 2012, captured the field conditions during a critical period of the 2012 midwestern drought. The lead author took oblique aerial photographs in the eastern and central two-thirds of Jo Daviess County during the drought of 2012. The photographs were taken in a high-wing aircraft from an altitude of 1,000 ft (305 m) during the summer, when bedrock crevice patterns were visible as vegetated crop lines. The Illinois Department of Transportation then took orthogonal aerial photographs in late August 2012 at our request, and we extracted images from Google Earth that were taken in September 2012. All three photographic methods revealed extensive vegetated crop lines in the thin soils overlying the creviced bedrock surface of the Galena Dolomite (Panno et al. 2013, 2015).

Lidar Elevation Data

Lidar elevation data were collected for Jo Daviess and adjacent Illinois counties during March 2009 as part of the Illinois Height Modernization Program (http://clearinghouse.isgs.illinois.edu/data/elevation/Illinois-height-modernization-ilmp-lidar-data). Lidar is a remote-sensing technique that uses a pulsing laser sensor to scan the earth's surface. The reflected light pulses are detected by instruments that record the location of each return pulse in three dimensions. After processing, lidar point cloud data provide a detailed three-dimensional elevation model of the surface (American Society of Photogrammetry and Remote Sensing 2002). The high-resolution elevation models produced from the approximately 1-m (3.2808 ft) horizontal point spacing lidar data provided detailed characterizations of sinkhole features, direct indicators of an associated underlying aquifer.

Ground-Penetrating Radar

Ground-penetrating radar, sometimes called georadar, ground-probing radar, or subsurface radar, uses electromagnetic waves to image materials underground that have contrasting electrical and magnetic properties. The technology is essentially the same as the traditional radar used to track airplanes, cars, and clouds, but instead of pointing the antennas into the air, they are pointed into the ground. The electromagnetic waves moving through the ground reflect off surfaces, layers (e.g., bedding), discontinuities (fractures), or objects that have contrasting electrical or material properties, and the sensor uses the returning echoes to create an image of the subsurface. In most soil and rocks, the depth of investigation varies from 3 to 30 ft (1 to 10 m), depending on the frequency of the radar instrument and the material properties of the ground. Ground-penetrating radar instruments use frequencies within the range of 10 to 1,500 MHz, overlapping the frequency range used by television and FM radio. Higher frequency instruments provide greater resolution, but with less depth of penetration. The ISGS operates a Noggin 250-MHz radar unit (Sensors and Software, Inc.) with an integrated global positioning system (GPS) system, which provides moderate penetration and moderate resolution in most rocks and soils. One of the main benefits of radar technology is the high lateral resolution of the images. The radar antenna is mounted on a four-wheeled cart, and a GPS antenna is mounted on a pole 6 ft (2 m) above the radar antenna. An odometer wheel attached to one of the rear wheels of the cart is used to trigger data acquisition every 3.8 in. (10 cm). A data logger records the output from the radar unit as well as positioning information from the GPS device. In this study, the GPS position was recorded once for every 10 radar traces. Later, this information was integrated into the same data file to produce images that were calibrated to GPS coordinates, and the elevation data embedded in the GPS information was extracted to provide topographic corrections to the radar images.

Field Observations

Previous fieldwork in the area was conducted in the mid-1990s by Weibel and Panno (1997) and Panno et al. (1997), and more recently by Panno et al. (2015). Fieldwork for this investigation was conducted across the county in agricultural fields; along streams where bedrock is exposed; and at road cuts, quarries, and natural outcrops. We examined the terrain for karst features, such as solution-enlarged crevices, sinkholes, caves, conduits, springs, and vegetated crop lines, as revealed by Panno et al. (2015). The orientations of vegetated crop lines and solution-enlarged crevices were determined relative to true north. All crevice orientation measurements in the field were determined by using a Brunton compass and corrected for magnetic declination by using current information from the National Centers for Environmental Information (2009). The magnetic declination for Nora, Illinois (eastern Jo Daviess County), at the times we were in the field was 1°32′ west of geographic north. All locations were determined by using a GPS system and were verified with aerial photography and lidar elevation models.

Groundwater Chemistry

Groundwater chemistry data from private wells and karst springs in eastern Jo Daviess County were available from the groundwater quality database of the Illinois State Water Survey (ISWS), as described in Panno and Luman (2008), and from Maas (2010), respectively. In addition, we sampled 10 private shallow wells across the county in June 2014 and one well in September 2013. All groundwater samples were analyzed for dissolved cations, anions, total Kjeldahl nitrogen (N), ammonia, nonpurgeable organic carbon, and the stable isotope ratios for water ($^{2}H/^{1}H$ and $^{18}O/^{16}O$,

reported in delta notation as δ deuterium [δD] and δ oxygen-18 [$\delta^{18}O$], respectively). All groundwater samples were analyzed for tritium content.

Wells were purged for at least 15 minutes until field parameters (temperature, pH, dissolved oxygen [DO], specific conductance, and oxidation–reduction potential) stabilized. The field parameters were analyzed with calibrated, parameter-specific probes (Hydrolab, Loveland, Colorado). Samples designated for chemical analyses were filtered through 0.45-µm membranes, placed in polyethylene or glass bottles, and stored at 4 °C before analysis. All samples were transported to the laboratory in ice-filled coolers and kept refrigerated until analysis. Analyses for inorganic chemicals were conducted in accordance with standard methods (American Public Health Association, American Water Works Association, and Water Environment Federation 1999) at the ISWS by using inductively coupled plasma spectroscopy and ion chromatography methods. Organic carbon was measured with a carbon analyzer.

Samples used for bacterial indicators (total coliforms and *Escherichia coli*) were collected by using sterile techniques. Outside spigots were flame sterilized. Water was collected in autoclaved glass bottles and stored in ice-filled coolers before transporting it to the analytical laboratory the same day. Bacterial indicators were determined by using the Colilert method (IDEXX Laboratories 2013) at the City of Dubuque Laboratory (Dubuque, Iowa).

Tritium was analyzed by using electrolytic enrichment (Ostlund and Dorsey 1977) and liquid scintillation counting as described in Hackley et al. (2007). Results are reported in tritium units (TU).

Water samples collected for stable isotope (δD and $\delta^{18}O$) analysis were filtered through a 0.45-µm filter and placed in high-density polyethylene bottles. The $\delta^{18}O$ values (using a modified CO_2-H_2O equilibration method), and δD values (using the zinc [Zn] reduction method) were determined by using a dual-inlet ratio mass spectrometer and were directly compared with an internal standard calibrated with international reference standards as described by Hackley et al. (2010). Results were reported in comparison with the international Vienna Standard Mean Ocean Water (V-SMOW) standard.

RESULTS AND DISCUSSION

Geology and Hydrogeology of Jo Daviess County

Because Jo Daviess County lies within the Driftless Area, for the most part, no glacial drift covers the bedrock, as is found in most of the upper Midwest in the United States (Figure 3). However, glacial till is exposed along U.S. Route 20 between the towns of Galena and East Dubuque (Willman and Frye 1970; D. Kolata, personal communication, 2014), as well as in a small area of glacial till in an isolated portion of the far eastern part of the county. Bedrock in the county consists of Middle Ordovician-age (443–490 million years ago [Ma]) carbonate rocks of the Galena and Platteville Groups, thin remnants of the Ordovician Maquoketa Shale, and Silurian (412–443 Ma) dolomite whose resistant rock caps the mounds and highlands of the county (Figures 2, 4, and 5).

Tectonic compression and extension occurred in this area during and after the formation of the Wisconsin Arch, which began in Cambrian time (490–543 Ma) and continued to be active in late Silurian or Devonian time (354–417 Ma; Nelson 1995). The Wisconsin Arch, in part, separates the Illinois Basin to the south from the Michigan Basin to the east. The Mississippi River Arch separates the Illinois Basin from the Forest City Basin to the west. Jo Daviess County lies on the southwestern flank of the Wisconsin Arch (Frankie and Nelson 2002; Figure 6). As a result of compression and extension, bedrock along the Wisconsin Arch has a well-developed vertical joint system. Heyl et al. (1959) stated, "All the rock formations in the [Upper Mississippi Valley mining] district [i.e., most of Jo Daviess County] contain well-developed vertical and inclined joints. The vertical joints are traceable for as much as 2 miles horizontally, and for as much as 300 ft vertically. Joints are especially well developed in the Galena dolomite" (p. 1). Heyl et al. (1959) identified three groups of joints: tension joints trending east–west to N 65° W, and two sets of shear joints trending N 20° to 30° E and N 20° to 30° W. Bradbury (1959) found that crevice orientations in numerous exposures in far eastern Jo Daviess County trend N 85° to 90° W and N 2° to 18° W. Trowbridge and Shaw (1916) stated that crevices within the Galena Dolomite "are frequently encountered in wells, and drilling tools are sometimes lost in them" (p. 57). The orientations of these features are consistent with findings by Panno et al. (2015) regarding vegetated crop lines. Panno et al. mapped 17,855 individual vegetated crop lines in Jo Daviess County during the drought of the summer of 2012 as a proxy for fractures and crevices. They found the dominant orientation to be nearly east–west and the subdominant orientation of the fractures and crevices to be nearly north–south.

Solution-enlarged crevices also acted as foci for ore mineralization in this area. Exceptionally large crevices (3 ft [1 m] wide) found in the Galena Dolomite, which were especially visible in quarries, were roughly oriented east–west and may be associated with this event. The Upper Mississippi Valley Zinc-Lead District, which includes Jo Daviess County and extends into Iowa and Wisconsin, is referred to as the Upper Mississippi Valley District. Heyl et al. (1959) and Bradbury (1959) have summarized the geology of this area. Lead (Pb)- and Zinc (Zn)-bearing ore minerals were mined in this area from the late 1700s until 1976 (Figure 7). Areas of primary ore mineralization called "gash-vein deposits" were found in solution-enlarged crevices (Figure 8) or in solution cavities in carbonate rocks of the Galena Group, although Pb-Zn mineralization was present within Cambrian through Silurian rocks. Galena (PbS_2) was the main ore mineral in these deposits, and sphalerite (ZnS_2) was the most abundant ore mineral associated with bedding planes and reverse faults (Heyl et al. 1959). Geochemical and isotopic indicators within the ore and associated minerals indicated that hydrothermal fluids (hypersaline brines) carrying Pb and Zn in solution were the source of the mineralization.

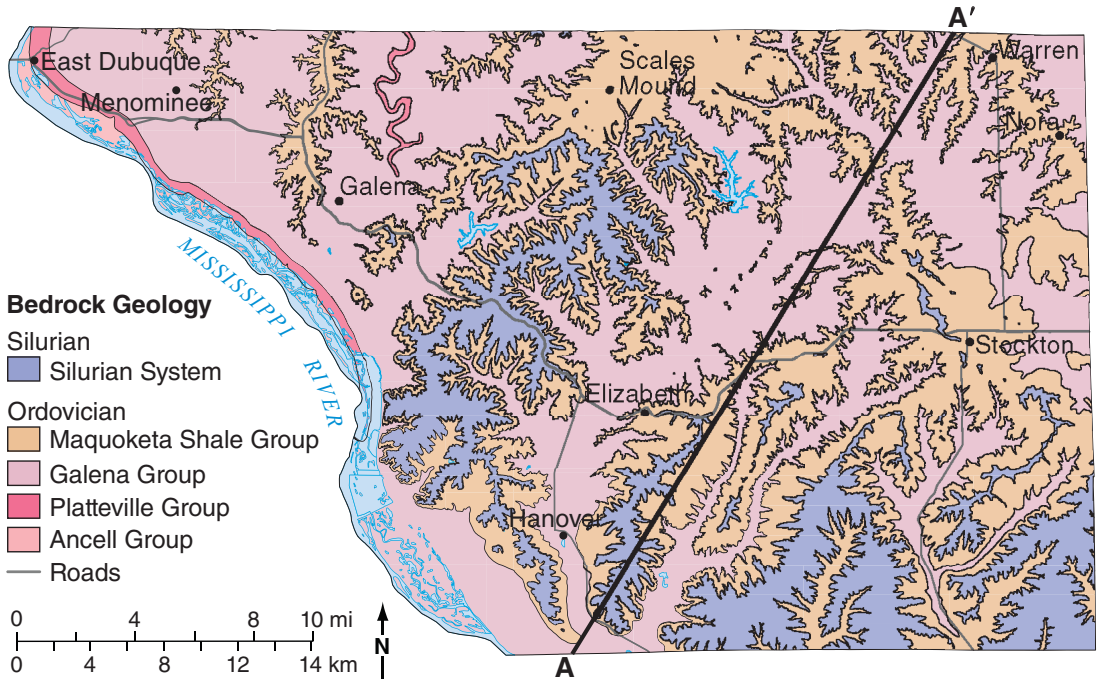

Figure 4 Generalized geologic map of Jo Daviess County (from Panno et al. 2014, 2016; modified from Kolata 2005). This is a reduced-scaled version of Map 1, which contains all the areas of interest examined or sampled within the county during this investigation.

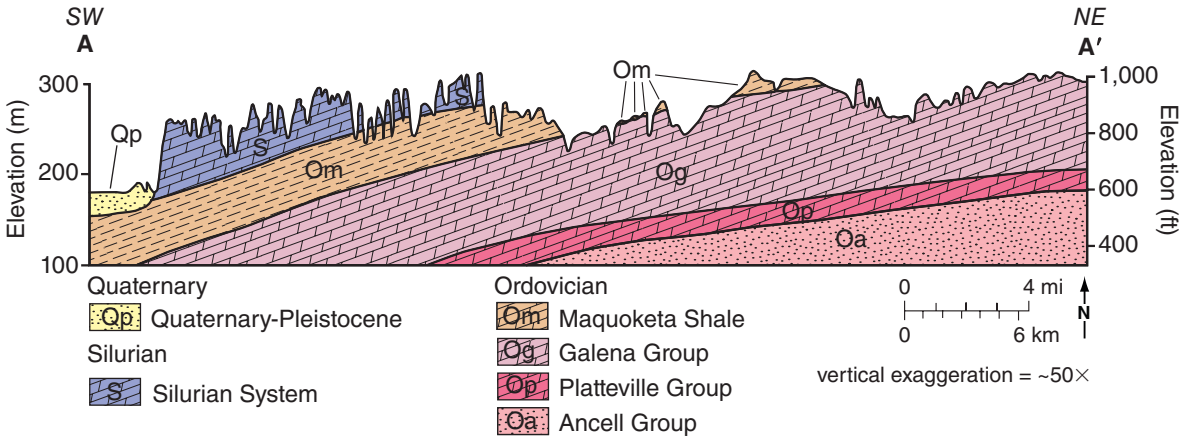

Figure 5 Cross section of northwestern Illinois showing dipping beds associated with the Wiconsin Arch and bedrock exposures (from Panno et al. 1997). The cross section line extends from the northwestern tip of Carroll County in the south to Warren, Illinois, in the far northeast (Figure 4). Data from Panno et al. (1997).

One of the more recent hypotheses proposed to explain the origin of these deposits (Rowan and de Marsily 2001) is that ore-forming solutions originated from evaporative brines associated with the Reelfoot Rift system (late Paleozoic time). Ore mineralization and dolomitization of the Ordovician carbonate rocks of this district have been dated as Early Permian in age (270 and 280 Ma; Brannon et al. 1992; Pannalal et al. 2004), suggesting early formation of solution-enlarged crevices by hydrothermal fluid throughout the study area.

Subsequent work by McGarry and Riggs (2000) identified most of Jo Daviess County as having "a very high aquifer sensitivity because fractured dolomite bedrock aquifers lie beneath the glacial drift or loess. Areas where dolomite bedrock is exposed are most sensitive" (p. 1). In addition, McGarry and Riggs (2000) characterized eastern Jo Daviess County as having a combination of both low (because of the presence of Maquoketa Shale) and very high sensitivities (because of exposed fractured dolomite bedrock) to groundwater contamination.

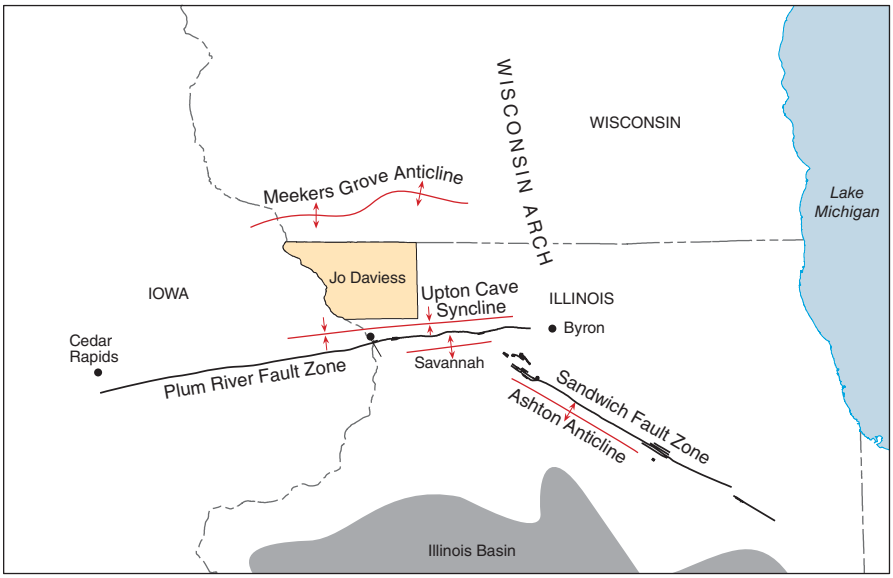

Figure 6 Structural features surrounding Jo Daviess County (highlighted in yellow; from Panno et al. 2014, 2015, 2016). Data from Nelson (1995).

In the mid-1990s, the ISGS identified the geology of Jo Daviess County as karst (Panno et al. 1997; Weibel and Panno 1997; see Figure 3). The main karst water-bearing formations in the county include the Galena and Platteville Groups. Silurian dolomite is also karstified but is rarely, if ever, used as an aquifer in the county. Panno and Luman (2008) examined sinkholes and the abundant secondary porosity (crevices) exposed along road cuts and in quarries in eastern Jo Daviess County and concluded that the Galena Dolomite constitutes a karst aquifer. They also showed that although sinkholes in the county were present, they were difficult to locate because of their relatively small size, owing to the thin soils. However, because of the presence of cover-collapse sinkholes associated with the Galena Dolomite, Jo Daviess County does fall into a "medium" to "high" category of aquifer vulnerability based on work by Lindsey et al. (2010) in other areas of the U.S. Midwest. Ekberg (2008) subdivided the secondary porosity of the Galena and Platteville Groups into matrix, fracture, and conduit porosity. These subdivisions are supported by spring hydrographs and drawdown curves from aquifer tests that support a triple-porosity aquifer. The fracture porosity through which groundwater flows consists of northeast- and northwest-trending vertical fractures (consistent with Heyl et al. 1959) and bedding planes (Ekberg 2008).

Vegetated Crop Lines

Because carbonate bedrock within the karst region of the Driftless Area in northwestern Illinois is typically overlain by unconsolidated deposits, including loess, direct observation of fractures and crevices has been restricted to infrequent occurrences of road cuts, quarries, and outcrops where bedrock is exposed at the ground surface. The sparse distribution of bedrock exposures has therefore made it difficult to develop a comprehensive understanding of the character and geometry of the primary carbonate bedrock aquifer within the region. However, extreme drought conditions in the U.S. Midwest during the summer of 2012 resulted in the formation of distinct lines and patterns predominantly in alfalfa fields planted in thin soils of the Driftless Area overlying the carbonate bedrock of Jo Daviess County (Figure 9a,b,c), the western portion of Stephenson County, and southern Wisconsin. Referred to as "vegetated crop lines" by Panno et al. (2013, 2015), the lines were created by denser, taller, and greener alfalfa plants aligned in 1- to 4-ft (0.3- to 1.2-m)-wide strips directly over buried bedrock fractures (Figure 9a,b,c). In Jo Daviess County, soil thickness ranges from bare bedrock to almost 25 ft (8 m; Riggs and McGarry 2000). During periods of drought, deep-rooted crops such as alfalfa can tap into the moist soil within the crevices and fractures of the underlying karst aquifer. Plants with roots in the crevices and fractures can thrive, whereas the adjacent plants fail to thrive because of the lack of water. No changes in elevation of the soil were observed in lidar elevation models of the crop-lined fields, indicating that this was a phenomenon created by the interaction of water-bearing bedrock crevices and vegetation only and not a topographic effect. This phenomenon provided a rare opportunity to indirectly examine the fractured and creviced buried bedrock surface of the Driftless Area and examine the connected porosity of the karst aquifer.

Using georeferenced aerial photography for 130 sites and digitizing each vegetated crop line in ArcGIS, we found that the nearly 18,000 digitized lines had predominantly east–west and north–south trends. A subset of the lines were oriented northeast–southwest and northwest–southeast. The east–west and north–south lines are consistent with fractures associated with the compression and extension of the Wisconsin Arch, whereas the northeast–southwest and northwest–southeast lines are consistent with shear zones (Panno et al. 2013, 2015). All the vegetated crop lines had orientations similar to the solution-enlarged crevices found in road cuts and quarries throughout Jo Daviess County, western Stephenson County, and northern Carroll County, as well as across the border into Wisconsin.

The presence of vegetated crop lines and their relationships with bedrock fractures and crevices observed in exposures (e.g., road cuts) indicate that the lines and patterns observed in the croplands are a direct reflection of the fractured and creviced pattern of the underlying karst aquifer in Jo Daviess County and adjacent counties. That is, the vegetated crop lines provide a road map of the secondary porosity that makes up the bedrock aquifer. These lines are useful in characterizing the aquifer and

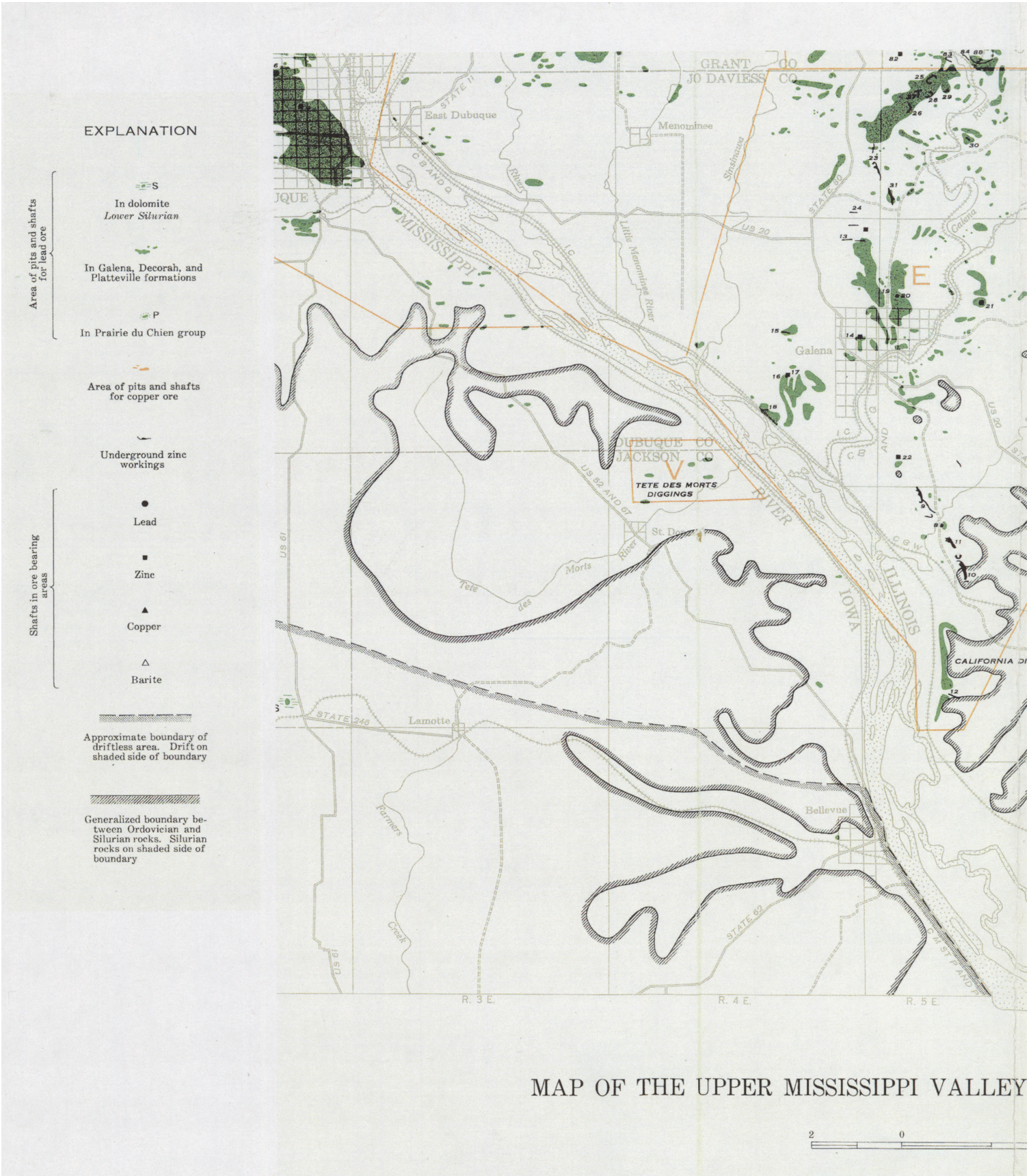

Figure 7 Map of the Upper Mississippi Valley Zinc-Lead District within Jo Daviess County (from Heyl et al. 1959). Mined areas are shown in green. Used courtesy of the U.S. Geological Survey.

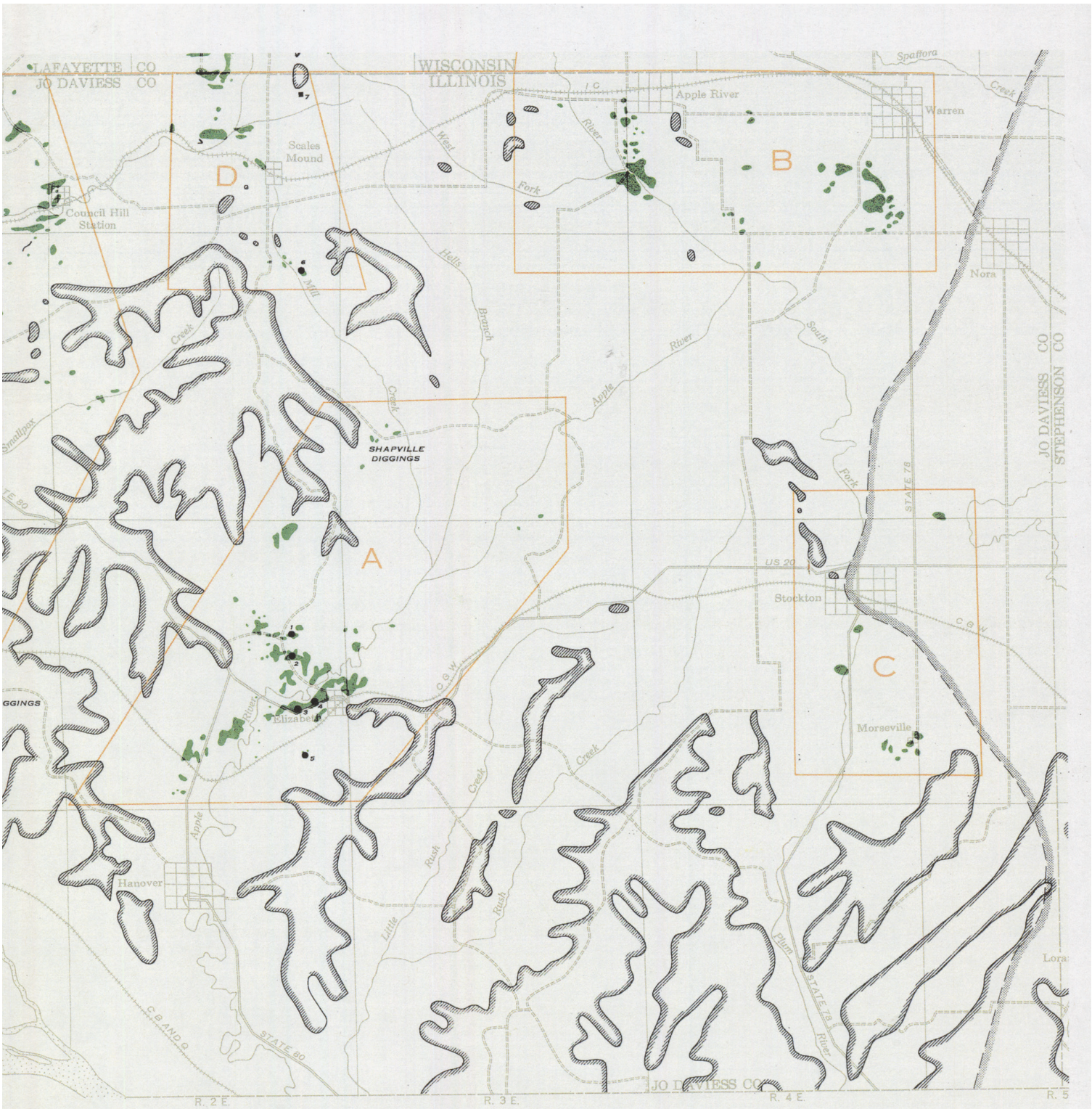

ZINC-LEAD DISTRICT, SHOWING LOCATION OF MINED AREAS

10 Miles

Figure 8 Solution-enlarged crevices are common karst features in northwestern Illinois and are exposed in road cuts, quarries, and outcrops. The crevice is located in a road cut along U.S. Route 20 just west of Freeport, Illinois. Photograph by Samuel V. Panno; used by permission.

for directing drilling for future hydrogeological and geochemical investigations. For example, a small sinkhole was observed in a lidar elevation model at the intersection of vegetated crop lines in the field in Figure 9b. A more detailed presentation of the vegetated crop line phenomenon in the Driftless Area of Jo Daviess County and a detailed comparison of the vegetated crop lines with crevices in exposures may be found in Panno et al. (2015).

Lidar Elevation Models

Close examination of detailed lidar bare-earth elevation model data revealed numerous cover-collapse sinkhole features developed in sediment overlying Silurian dolomite in western Jo Daviess County (discussed below; see Map 1) However, fewer sinkholes were observed for lidar elevation data where creviced Galena Dolomite is overlain by thinner loess soils and in places where thick sequences of Maquoketa Shale are present. The relative paucity of sinkholes in this formation is primarily because sinkholes in sediments overlying the Galena Dolomite tend to be smaller than the resolution of the lidar (4 ft [1.2 m]), or they were filled with residual snow when the lidar was collected (March 2009) and were not visible (Panno and Luman 2008), or both. Consequently, the focus of our investigation was the relationships among cover-collapse sinkholes

Figure 9 Crop lines in an alfalfa field in eastern Jo Daviess County during July 2012 as seen (a) from the ground and (b) oblique from the air (from Panno et al. 2013, 2015). Photographs by Samuel V. Panno; used by permission. (c) Crop lines in an alfalfa field in eastern Jo Daviess County in August 2012 as seen from Google aerial photography (from Panno et al. 2013, 2015); © Google Earth. The locations of photographs are shown on Map 1.

and solution-enlarged crevices visible in road cuts and quarries, and their relationships to vegetated crop lines and to the fracture traces seen in quarry floors.

Silurian Dolomite

Examination of the lidar elevation models revealed numerous cover-collapse sinkholes in western Jo Daviess County overlying Silurian dolomite (Figure 10). Examination of the area on the ground revealed numerous sinkholes, solution-enlarged crevices, and small caves (Figures 10, 11, and 12). Crevices in the Silurian dolomite are relatively wide (up to 3 ft [1 m] or more;

Figure 10 (a) Cover-collapse sinkholes in unconsolidated sediment overlying creviced Silurian dolomite in a contoured lidar elevation model (contour interval = 5 ft [1.5 m]; from Panno et al. 2014, 2016; Map 1). Map by Donald E. Luman. (b) A 3-ft (1-m)-wide crevice in Silurian dolomite, oriented in an east–west direction and located in a road cut across from the Long Hollow Scenic Overlook located between Galena and Elizabeth, Illinois (from Panno et al. 2014, 2016; Map 1). Photograph by Samuel V. Panno; used by permission.

Figure 11 Cover-collapse sinkholes in unconsolidated sediment overlying creviced Silurian dolomite. The cover-collapse sinkholes are (a) near Chestnut Mountain Resort south-southwest of Galena (from Panno et al. 2014, 2016; Map 1), and (b) within the Mississippi Palisades State Park just south of the Jo Daviess County line along the Mississippi River. Photographs by Samuel V. Panno; used by permission.

Figure 10). Sinkholes in this area are nearly circular features 6 to 21 ft (2 to 7 m) deep and 60 to 100 ft (20 to 30 m) in diameter (based on measurements of lidar elevation data; Figure 10). Weibel and Panno (1997) and Panno et al. (1997) examined several of the sinkholes initially seen in aerial photographs. Many more sinkholes were detected by direct inspection of lidar bare-earth elevation model data, and most of the sinkholes are aligned along nearly east–west-trending (N 80° W) lineaments in sediment overlying Silurian dolomite (Figure 10). Weibel and Panno (1997) and Panno et al. (1997) reported that they are collapse features, with no evidence of waste piles that would suggest excavations. Consequently, they were sinkholes and not small-scale mining operations that followed veins of ore minerals (locally referred to as "sucker holes"; Figure 13). Although a large sinkhole area is in the vicinity of the "California diggings" (Map 1) in the far southern edge of the Galena subdistrict (Heyl et al. 1959), the ore deposits in this area

Figure 12 A 3-ft (1-m)-diameter conduit within Silurian dolomite showing the development of frost as a result of warm, moist air discharging from the entrance. Other similar conduits were present at this location at the base of dolomite blocks sliding on Maquoketa Shale and reveal the presence of phreatic brachwork-type conduits and caves along the Maquoketa Shale-Silurian dolomite contact. The site is located just west of Elizabeth, Illinois (Map 1). Photographs by Elizabeth L. Baranski; used by permission.

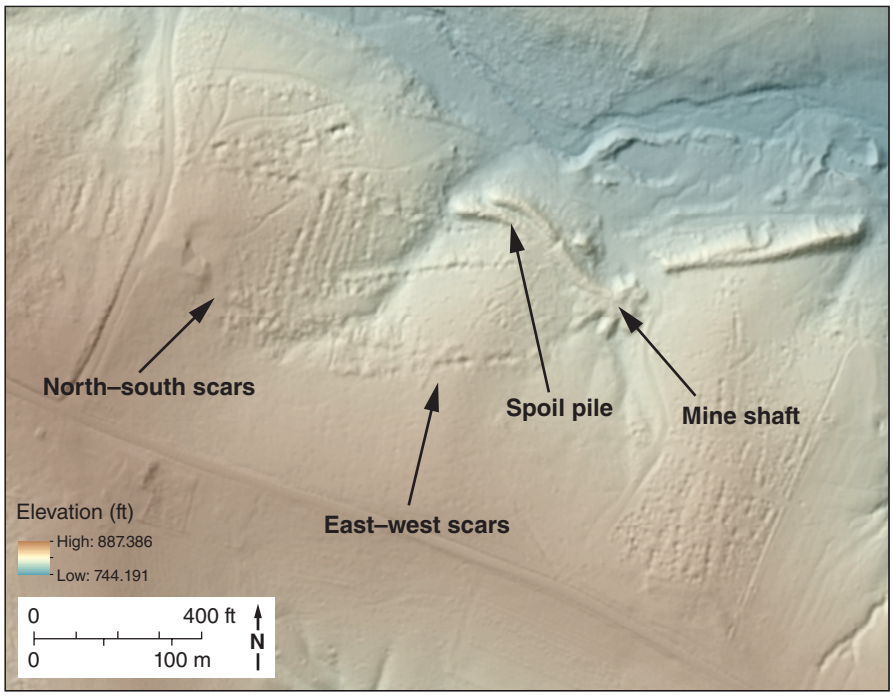

Figure 13 Mining scars in Galena Dolomite from the Vinegar Hills Mine area just north of Galena, Illinois, as seen in a lidar bare-earth elevation model showing linear excavations from zinc–lead mining that appear as east–west-trending holes. The miners followed mineralized crevices. The holes range from 3 to 25 ft (1 to 8 m) in diameter (Map 1). Map by Donald E. Luman.

are primarily within the deeper Galena Dolomite underlying the Silurian dolomite and Maquoketa Shale. More than 100 of these sinkholes were examined by using the lidar bare-earth elevation model data, whereas only about 10 of these Silurian dolomite sinkholes were examined in the field and found to be cover-collapse sinkholes. A few of these features could possibly be related to subsidence caused by adjacent large-scale mining operations (e.g., Touseull and Rich 1980).

Road cuts in the area between 3 and 4 mi (5 and 8 km) east of the California diggings (Map 1) revealed that these aligned sinkholes probably formed along nearly east–west-trending crevices that range from 1.5 to 3 ft (0.5 to 1 m) in width (Figure 10). The crevices at this site are at least 20 ft (6 m) below land surface, as seen in road cuts, and they truncate at the Maquoketa Shale. The collapse of sediment into these large crevices probably created the aligned sinkholes observed in the lidar bare-earth elevation models. In addition, many large blocks of Silurian dolomite on ridges have been observed to separate along crevices and migrate downhill, "sliding" on the underlying shale (Figure 14). This movement results in the dilation of existing crevices, thereby creating the relatively large aligned collapse features (Panno et al. 2014).

Because the Silurian dolomite is of limited areal extent and forms the highlands of Jo Daviess County, it is rarely used as a groundwater source in this area, although it does serve as an important aquifer in other counties of Illinois

Figure 14 A tilted block of Silurian dolomite along a highland slowly sliding downhill on Maquoketa Shale. The site is located just west of Elizabeth, Illinois (from Panno et al. 2014, 2016; Map 1). Photograph by Elizabeth L. Baranski; used by permission.

Figure 15 Spring within the Hanover Bluff Nature Preserve discharging from an 0.8-in. (2-cm)-wide crevice near the base of the Silurian dolomite (far right). The discharge rate was about 0.05 L/s (Map 1). Photograph by Samuel V. Panno; used by permission.

(e.g., Will County in northeastern Illinois). However, springs near the base of the Silurian dolomite are common throughout Jo Daviess County. This is due to recharge into the dolomite via sinkholes and crevices entering crevice caves and conduits underlain by Maquoketa Shale. Here, groundwater flows laterally along the dolomite–shale contact and discharges as a spring along the slope where the two formations are exposed (Figure 15). Property owners use some of these springs as their primary water source.

Ordovician Galena Dolomite

The karst expression of the Ordovician Galena Dolomite consists of relatively narrow fractures 0.04 to 0.35 in. (1 to 9 mm) wide and crevices typically 3 to 4 in. (8 to 10 cm) to 1 ft (30 cm) wide, with some up to 3 ft (1 m) wide observed in road cuts and quarries (Figures 8, 16, and 17). Crevice- or network-type caves are also found in Galena Dolomite, but they tend to be dry, with few if any speleothems and are of limited extent (Figure 18a). Because of the relatively thin soils overlying the Galena Dolomite, sinkholes are smaller and less noticeable than those of the Silurian dolomite in the county. Cover-collapse sinkholes in sediment overlying Galena Dolomite range from 3 to 10 ft (1 to 3 m) in diameter (Figure S5 in Panno and Luman 2008; Figure 18b), and, because of their sizes, are difficult to delineate on lidar elevation models. Because of the ubiquitous nature of row-crop agriculture in this area, sinkholes are typically obscured by farming practices and are found intact only in pastures and undeveloped ground. However, some oriented drainage traces leading to streams are the result of soil and sediment collapsing into underlying crevices. Cover-collapse sinkholes overlying the Galena Dolomite in nearby southeastern Minnesota open frequently and are filled in by landowners within several days (J.A. Green, Minnesota Department of Natural Resources, personal communication, 2014).

Springs and spring morphology in Jo Daviess County are characteristic of karst in that springs are often found in relatively large (15- to 21-ft [5- to 7-m]-diameter) cusp-shaped or semicircular depressions resembling sinkholes, with an outlet leading to a stream (Figure 19). Stream morphology is similarly distinct in that many stream valleys are linear, with sharply angular meanders (Figure 20). These angular features are classic geomorphologic features known as trellised drainage patterns and indicate bedrock control of the streams in Jo Daviess County; that is, water tends to flow along the fracture or crevice traces, which represent zones of enhanced weathering in the bedrock surface. These sharp angles have orientations similar to those of the mapped crevices, vegetated crop lines, and fracture traces, and they reflect bedrock control. All these features are a result of the joint-controlled fabric or pattern of the underlying karst aquifer, as seen in vegetated crop lines and bedrock exposures (Panno and Luman 2008; Panno et al. 2013, 2015). Vegetated crop lines identified by Panno et al. (2015) in the study area reveal the character, density, and extent of these features in much greater detail than in road cuts and quarries.

Ground-Penetrating Radar

Crevices observed in road cuts and quarries near Warren and Nora, Illinois, were investigated with GPR to help determine their depth in the subsurface. This was done to ascertain whether these features are part of the porosity of the karst aquifer or are merely near-surface features. We used GPR to examine the condition of the bedrock on both sides of Illinois Route 78 near an outcrop across the street from an abandoned quarry. Two crevices were evident in

Figure 16 Photomosaic of a road cut located just east of Elizabeth, Illinois, along U.S. Route 20, Jo Daviess County (looking south), showing solution-enlarged crevices in the Galena Dolomite. Orientations on the photograph are those obtained at the road cut by using a Brunton compass (Map 1). Photographs by Samuel V. Panno; used by permission.

the outcrop on the east side of the road (Figure 21). The GPS positions allowed us to locate features accurately on both sides of the road. After topographic corrections were applied, the radar revealed several vertical discontinuities on both sides of the road. The crevices accounted for two of these discontinuities on the east side. The southernmost crevice was more prominent in both the surface and subsurface expression. Both discontinuities could be traced to similar features on the west side of the road. At least four other discontinuities could be traced from the east to the west side of the road. It is likely that groundwater drainage to the quarry suppresses the water table and enhances the radar penetration. This results in radar signals of larger amplitude along this stretch of the road. The crevices were observed to depths of at least 15 ft (3 m) from the top of the road cut, and they probably extend deeper into bedrock.

We also examined a farm just south of Warren (Figure 22), where vegetated crop lines had been observed (by the owner) on a west-facing slope on the farm during the dry summer months. This observation suggested the presence of fractures or crevices just below the soil zone from which crops were obtaining water. To investigate this possibility, we acquired a series of north–south-trending GPR profiles along this slope. The three GPR profiles (lines 8, 9, and 11) were separated by about 30 ft (10 m) and followed the contour of the slope in the area indicated by the owner (Figure 22). Minimal processing of the radar data included gain adjustments and topographic corrections using integrated, low-resolution GPS signals. For presentation of the data, line 8 has been reversed and lines 8 and 9 have been stretched to visually align with line 11. Subhorizontal layering, either soil or rock, is apparent in all three lines; the depth to bedrock is <3 ft (1 m). Vertical anomalies and discontinuities in this layering are indicated in Figure 23. These discontinuities are fractures based on vegetative crop line data in the area (Panno et al. 2015). They are very numerous in lines 8 and 9 but less numerous in line 11 farther downslope. Many of the fractures on lines 8 and 9 appear to align from line to line, although the large spacing between the two lines prevents definitive identification of individual fractures. Some of the apparent vertical anomalies in the radar data may be the result of surface roughness in the field and may not necessarily be indicative of subsurface fracturing. However, several anomalies are similar to ones imaged along the road, where they were clearly associated with fractures. The abundance of vegetated crop lines observed by Panno et al. (2015) suggests that the features in GPS profiles are near-vertical fractures and crevices within the bedrock.

Bedrock Exposures in Road Cuts and Quarries

Open crevices visible in road cuts and quarries in Jo Daviess County and adjacent counties are common features in the Silurian dolomite and Galena Group (Figures 8, 10, 16, and 17). These features are often referred to as "cutters" or "grikes" (White 1988). Howard (1963) first called these features cutters and reasoned that they were one of three morphological features that characterized karst areas in temperate climates (the other two being sinkholes and caves). Pluhar and Ford (1970) described two types of cutters: the "cleft karren" and the "trench karren." Cleft karrens are characterized as linear, open fractures and crevices that continue below the surface and slowly narrow with depth. These features provide pathways for surface water (rainwater and snowmelt) to enter the subsurface and are seen in both the Galena Group and Silurian dolomite. Trench karrens are characterized as sinuous, open joints or crevices that extend down to and terminate at a resistant bed; in the case of Silurian dolomite, pseudo trench karren characteristics are seen along ridge tops, where large blocks are sliding on the underlying resistant bed, the Maquoketa Shale.

Surface and near-surface exposures of solution-enlarged crevices in road cuts and quarries typically contain fine sediment derived from overlying soil and associated materials (e.g., residuum, residual Maquoketa Shale for Galena Dolomite) that wash into the crevices during rainfall and snowmelt events. However, below the water table, hydrostatic pressure and the movement of groundwater can mobilize and periodically flush this material from the crevices; this action provides open conduits for groundwater flow. Karst aquifers are well known to be highly dynamic, and sediments within the aquifer are ephemeral in their nature (M. Field, U.S. Environmental Protection Agency [USEPA], personal communication, 2009). To use a sinkhole pond as an example, conduits at the base of sinkholes in Illinois' sinkhole plain in southwestern Illinois can become plugged with fine sediment and form ponds. Eventually, a large rainfall event can raise the level of the sinkhole pond to the point at which hydrostatic pressure forces water past the sediment plug, rapidly eroding the plug through a phenomenon known as piping. Once the sediment plug is compromised, the pond quickly drains (e.g., Panno et al. 1999). Another example is periodically flooded caves, where some crevices may be filled while others remain open, a "dynamic process" in which some crevices are active parts of the karst aquifer network and some are not and their status is changing with time (C. Alexander, University of Minnesota, personal communication, 2009).

Several examples of crevices in dolomite that have been exposed by road cuts and quarries in Jo Daviess County are described below. Measurements of crevice orientation along road cuts ranged from difficult to problematic because of erosion and dense vegetation.

Savanna Blacktop and Quarry

In a photograph of an exposure of Galena Dolomite at the Savanna Blacktop and Quarry in Carroll County, located just south of Jo Daviess County and 2 mi (3 km) southeast of Savanna, Illinois, the exposure is 30 to 50 ft (10 to 15 m) above the water table (Frankie 2001; Figure 23). Crevices as large as 3 ft (1 m) wide have been observed extending 9 ft (3 m) or more below ground surface and appearing to narrow abruptly with depth. The widths of these crevices near the bottom of the quarry are about 1 in. (2.5 cm; W. Frankie, ISGS, personal communication).

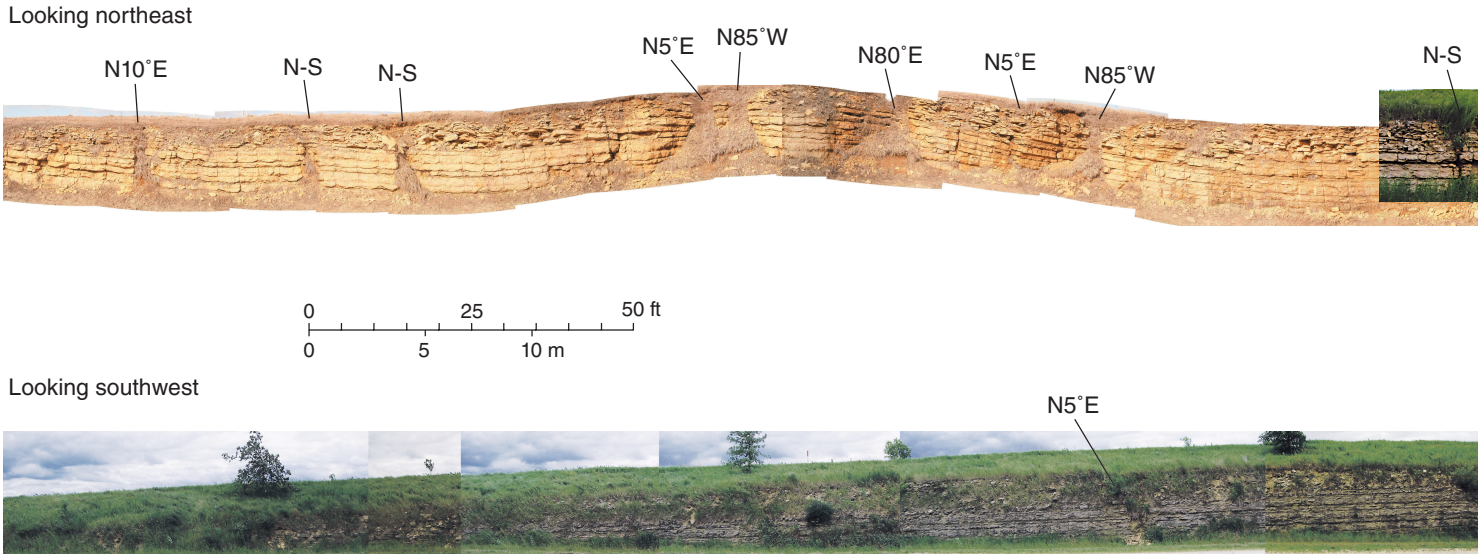

Figure 17 Photomosaic of a road cut (both sides of the road) located on Illinois Route 78 just southeast of the Wisconsin border (Map 1), showing abundant solution-enlarged crevices in the Galena Dolomite. Orientations on the photograph are those obtained by using a Brunton compass. Photographs by Samuel V. Panno; used by permission.

Figure 18 (a) Cave within Galena Dolomite just east of Elizabeth, Illinois. This cave is about 3 ft (1 m) wide and the floor is made up of fine-grained sediment. (b) Cover-collapse sinkhole in unconsolidated material overlying Galena Dolomite in eastern Jo Daviess County. Sinkholes overlying this formation are relatively small because of thin soils. Photographs by Samuel V. Panno; used by permission.

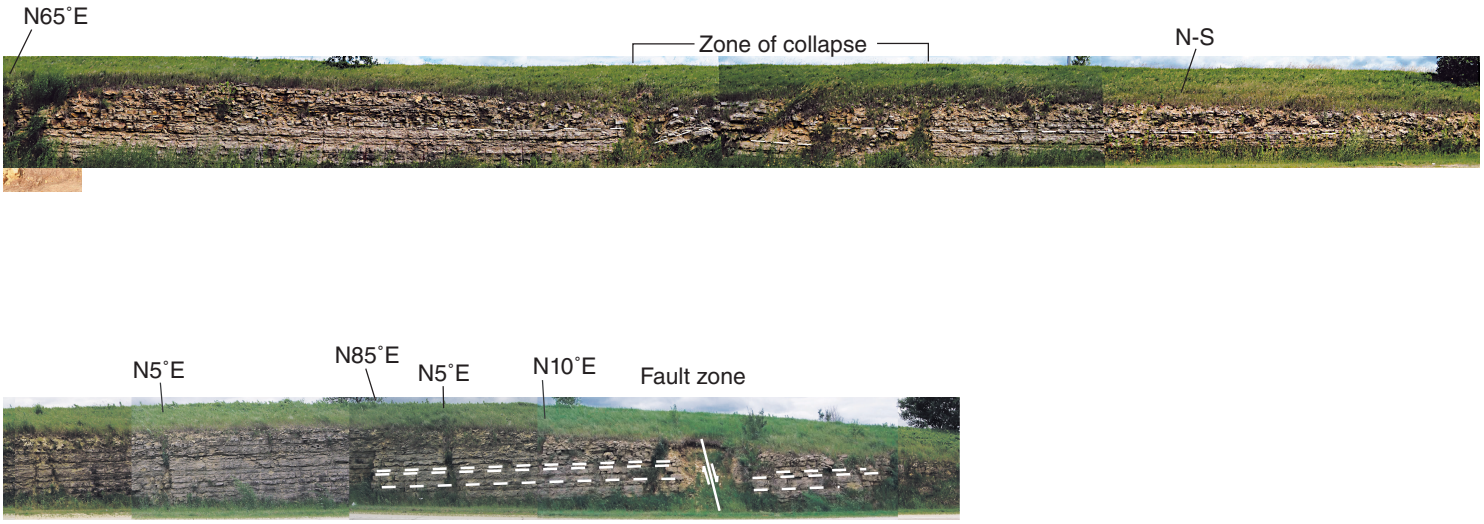

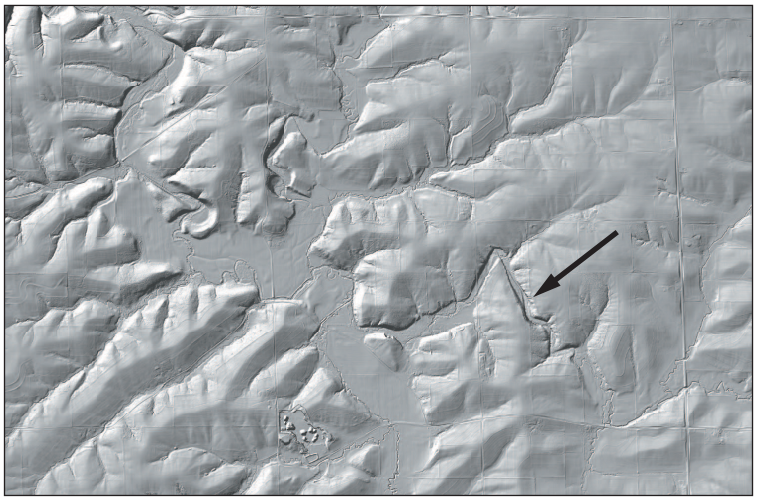

Figure 19 A karst spring discharging from a crevice at the base of the tree within the Galena Dolomite and draining off to a nearby stream (from Panno et al. 2014, 2016; Map 1). Photograph by Samuel V. Panno; used by permission.

Figure 20 Angular stream channel (see arrow) as revealed on a lidar bare-earth elevation model showing bedrock-controlled, angular stream geometry within the Galena Dolomite (Map 1, Other Feature). Map by Donald E. Luman.

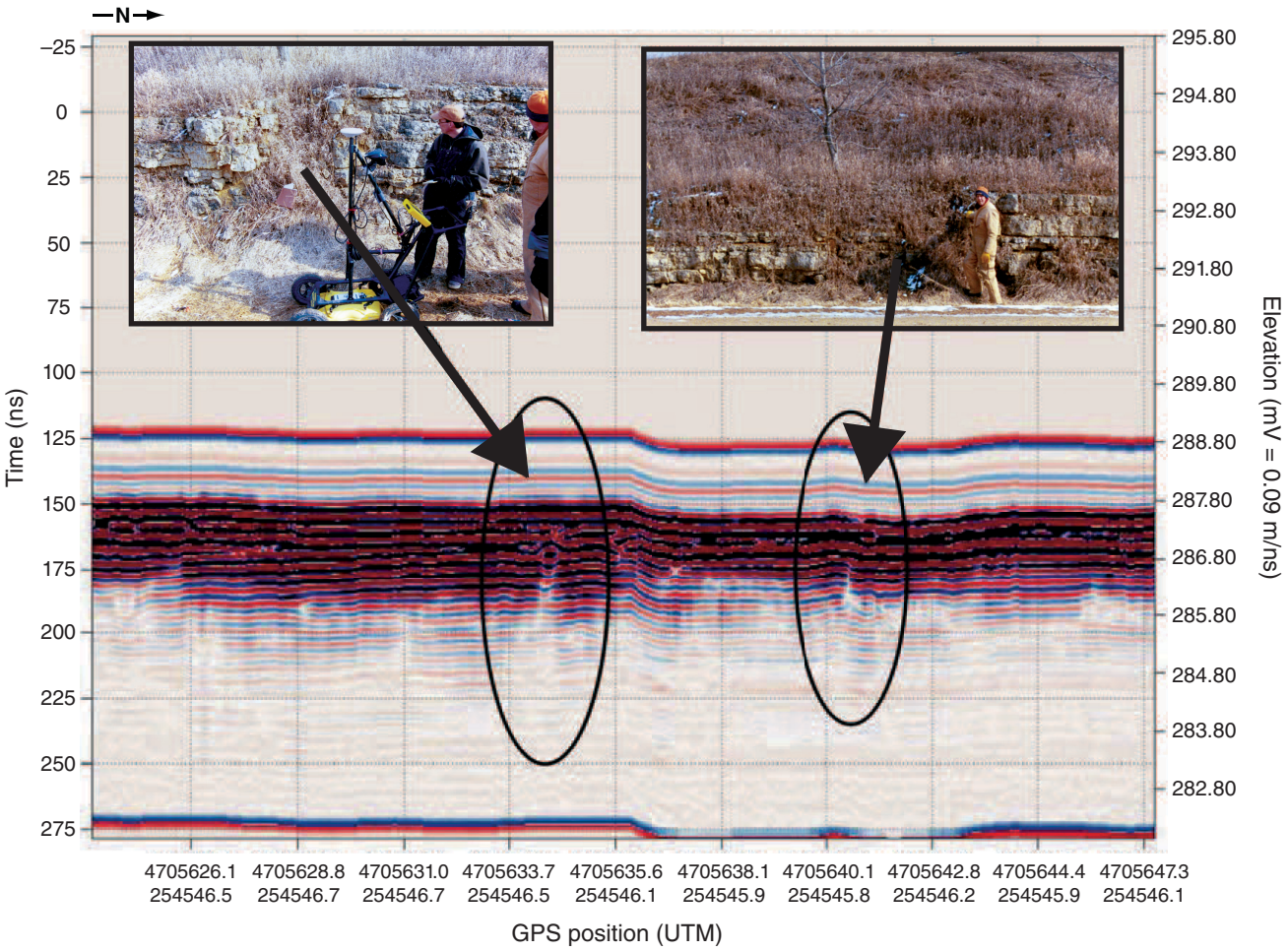

Figure 21 Ground-penetrating radar (GPR) locations of and data on crevices within the Galena Dolomite exposed within a road cut along Illinois Route 78 just south of Warren, Illinois (Map 1). The GPR data revealed the openness of the crevices. Photographs by Samuel V. Panno; used by permission.

Illinois Route 78 Road Cut (near the Wisconsin Border)

A road cut along the northernmost part of Illinois Route 78 just south of the Wisconsin border has exposed a relatively long portion of the Galena Dolomite. This road cut contains abundant fractures, crevices, and other geologic features. The locations and orientations of each crevice were mapped and measured (Figure 17). Two faults were identified along this road cut, one with about 6 ft (2 m) of displacement and the other with about 6 in. (15 cm) of displacement (Figures 24 and 25). Dominant crevice orientations along this road cut are roughly north–south and east–west. These orientations are consistent with vegetated crop lines (Panno et al. 2015) found in the field above the north side of the road cut, where crop lines intersect crevices within the road cut (Figure 26). Another feature at this road cut includes a 50-ft (15-m)-wide collapse zone that contains rotated blocks, one of which appears to have dropped vertically by as much as 8 ft (2.5 m; Figure 27). No displacement of bedding was observed on either side of this collapse zone. The collapse zone may suggest the presence of an underlying cave or conduit.

U.S. Route 20 Road Cuts

Numerous crevices in Silurian dolomite were present in a road cut across the highway from the Long Hollow Scenic Overlook, with the most prominent being 2 to 3 ft (0.6 to 1 m) wide and oriented in a nearly east–west direction (Figure 10b). Similarly, cover-collapse sinkholes overlying Silurian dolomite are aligned and follow large crevices that trend east–west and are best seen in lidar elevation models (Figure 10a). On the ground, sinkholes are found almost exclusively in wooded areas and range from 30 to 60 ft (10 to 20 m) in diameter (Figure 11a,b). Field examination of sinkholes near Chestnut Mountain Resort, located south of Galena, revealed that a tangle of vegetation in most of the sinkholes made exploration of the depths of the sinkholes nearly impossible. However, the penetrating nature of lidar made it possible to determine the depth of these sinkholes, which are 10 to 15 ft (3 to 5 m) deep (Figure 10a).

A road cut located just east of the Apple River on U.S. Route 20 contained east–west-oriented crevices about 2 in. (5 cm)

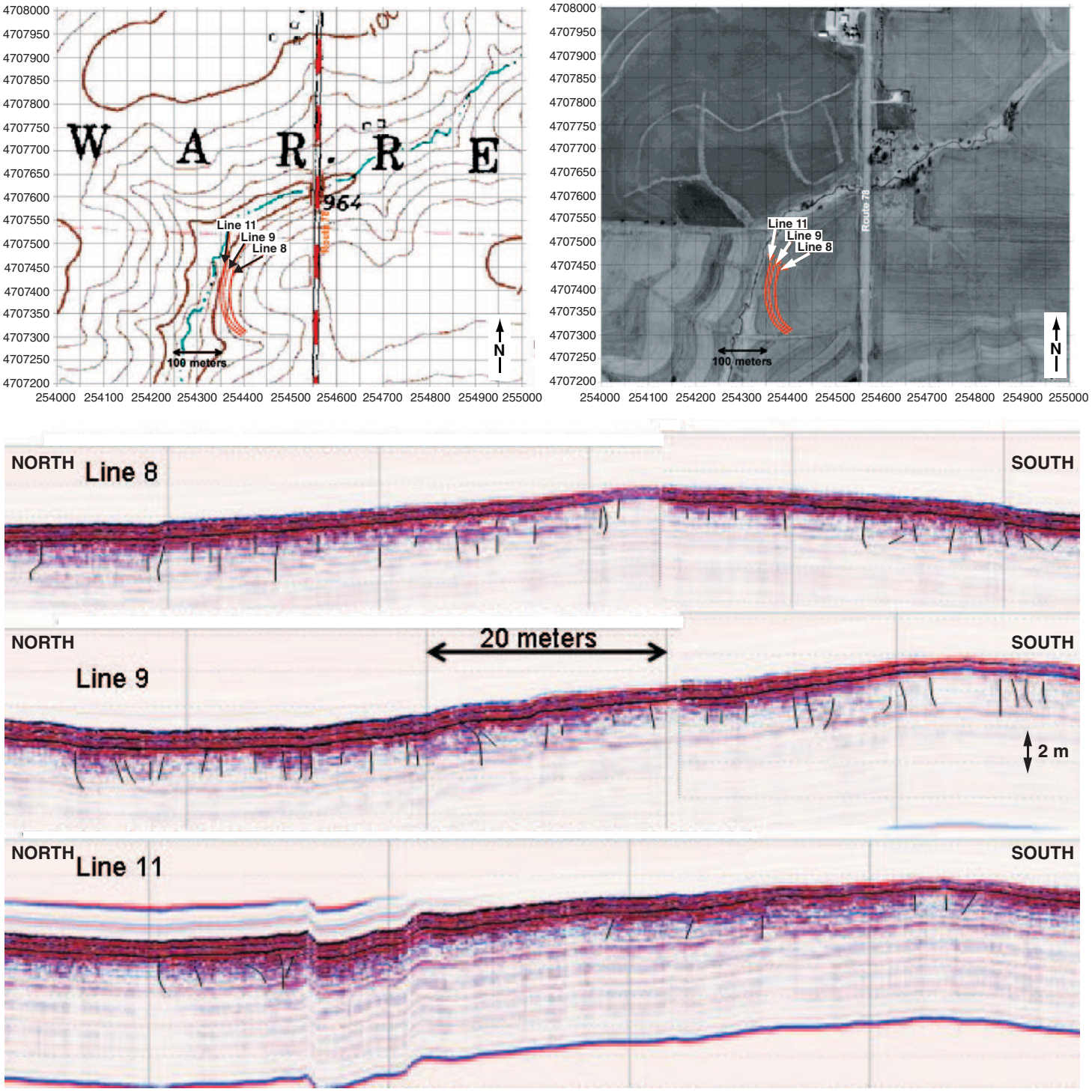

Figure 22 Ground-penetrating radar (GPR) location and data, and an aerial photograph of a field located just south of Warren, Illinois (Map 1), showing multiple fractures and crevices within a field. Again, GPR revealed the openness of the fractures and crevices. Topographic map and aerial photograph courtesy of the U.S. Geological Survey.

Figure 23 Working face of the Savanna Blacktop and Quarry located just south of the Jo Daviess County border in Carroll County (from Frankie 2001). Photograph by Wayne T. Frankie.

wide. West of the river on U.S. Route 20 and just east of the town of Elizabeth, Illinois, a road cut revealed more Silurian dolomite containing two wide crevices, each 3 ft (1 m) wide and oriented in an east–west direction (Figure 16). The orientation of one very wide zone (6 to 10 ft [2 to 3 m]) could not be determined. Two smaller crevices were oriented N 30° E (6 in. [2.4 cm] wide) and N 15° W (2 in. [5 cm] wide). This exposure also contained well-preserved Halysites coral, which is an index fossil of Silurian dolomite.

Louis' Aggregate Stockton Quarry

This quarry is located about 2.5 mi (4 km) south-southwest of Nora, Illinois. It was examined in 2008 (Figure S1 in Panno and Luman 2008) and was revisited on June 30, 2009. Crevices in this quarry were oriented roughly east–west (Figure 28a) and north–south (Figure 28b). The east–west-trending crevices were widest and ranged from 3 ft (1 m) wide (the entire exposure) to one that was 1.5 ft (0.5 m) at the quarry top and less than 0.4 in. (1 cm) at the bottom (quarry depth was approximately 35 ft [11 m]; Figure 28a). In addition, the south quarry face showed fresh blast damage that consisted of vertical zones of discolorations about 1 ft (0.3 m) wide (Figure 29). These blast features highlight the limited nature of blast damage and their distinct difference from fractures and crevices in road cuts and quarries.

Civil Quarry

Civil Quarry is located about 4 mi (6.5 km) north of Stockton and contains one large east–west-trending crevice (3 ft [1 m] wide and about 25 ft [7.5 m] deep). The rest of the exposures in the quarry revealed abundant fractures but few crevices. One location revealed three equally spaced crevices that are about 1 in. (2.5 cm) wide and oriented in an east–west direction (Figure 30).

Crawford Quarry

Located in southwestern Jo Daviess County just south of the Hanover Bluff Nature Preserve, Crawford Quarry provides an excellent exposure of Silurian dolomite. The quarry floor contains abundant fracture or crevice traces highly visible in aerial photographs (Figure 31). These fracture traces are identical in spacing and orientation to those of vegetated crop lines discussed below and represent the fracture and crevice geometry of the Silurian dolomite, which is essentially the same as that of the underlying Galena and Platteville Groups.

Good Miller Quarry

Good Miller Quarry is located south of Stockton, Illinois, in Jo Daviess County and is in Silurian dolomite. The quarry walls (about 60 ft [18 m] high) contain abundant fractures and solution-enlarged crevices (Figure 32). The width of the crevices tends to narrow with depth, and most are filled with fine-grained sediment at and near the surface. However, near the base of the quarry wall, several of these crevices appear to be connected to or are immediately adjacent to open crevices of limited height (3 to 6 ft [1 or 2 m]) and open conduits (Figure 32). The water table is below the quarry floor and at the time of our visit, at least one groundwater seep was visible on the quarry floor.

Figure 24 Detail of a fault zone on the southwestern side of the Illinois Route 78 road cut (Map 1) showing a displacement of about 6 ft (2 m). Photograph by Samuel V. Panno; used by permission.

Figure 25 Detail of a fault zone on the northwest side of the Illinois Route 78 road cut (Map 1) showing a displacement of about 6 in. (15 cm). Photograph by Samuel V. Panno; used by permission.

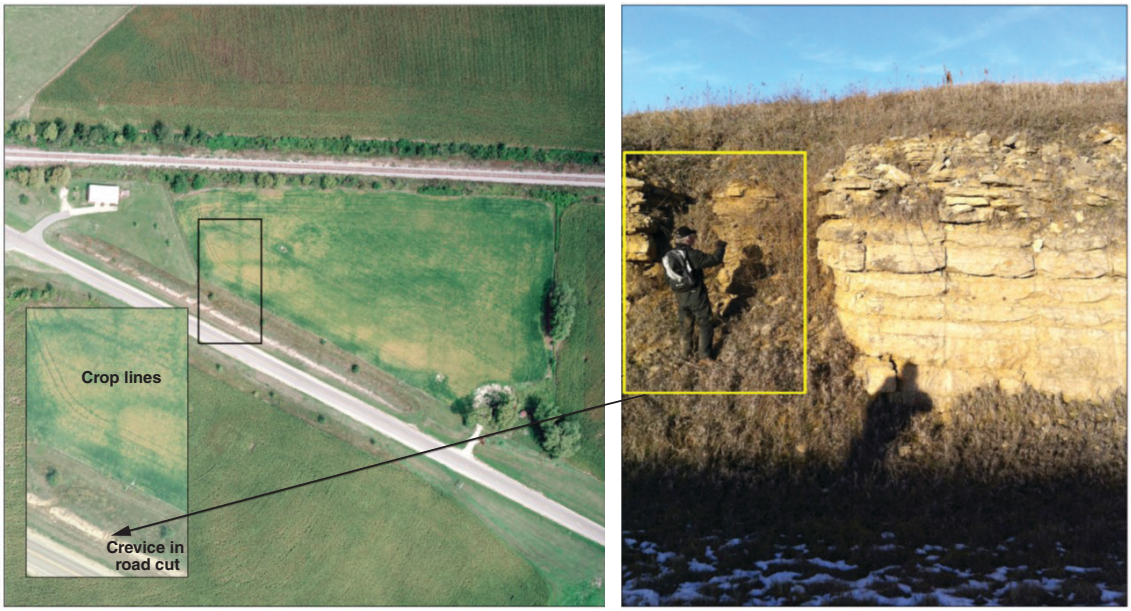

Figure 26 Alignment of crop lines (left) with crevices in a road cut (right; Map 1). Aerial photograph (left) by the Illinois Department of Transportation. Ground-based photograph (right) by Donald E. Luman; used by permission

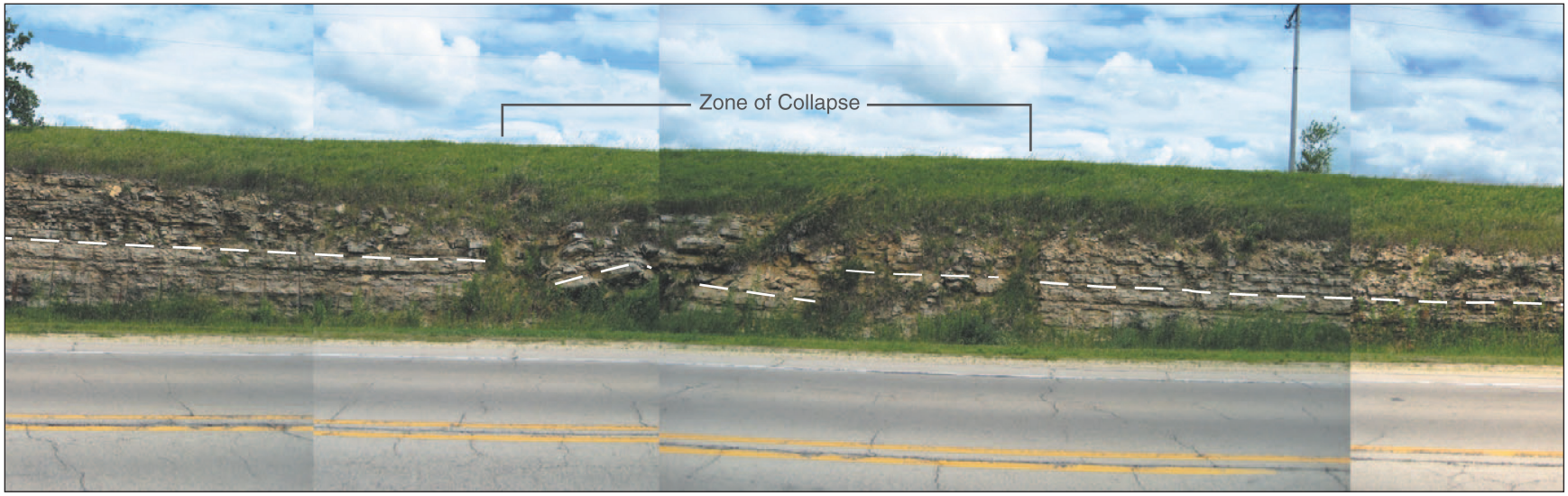

Figure 27 Detail of a collapse zone on the northeastern side of the Illinois Route 78 road cut (Map 1). The collapse zone is about 50 ft (15 m) wide at this exposure. Photographs by Samuel V. Panno; used by permission.

Figure 28 (a) Crevice trending east–west in a wall of the Louis' Aggregate Stockton Quarry (Map 1). The width of the crevice goes from about 6 in. (15 cm) near the top to about 1 in. (0.4 cm) near the bottom. The height of the exposure is about 21 ft (7 m). (b) Crevice trending north–south and filled with fine-grained sediment within the Louis' Aggregate Stockton Quarry with a gob pile in the foreground. The height of the exposure is 13 ft (4 m). Photographs by Samuel V. Panno; used by permission.

Figure 29 Blast damage in a working face at the Louis' Aggregate Stockton Quarry (Map 1). The height of the face is about 35 ft (11 m). Notice the subtle nature of these features (arrows) compared with the well-defined crevice shown in Figure 28. Photograph by Samuel V. Panno; used by permission.

Figure 30 Three east–west-oriented crevices in the working face of Civil Quarry (Map 1). These crevices had a width of about 0.5 to 1 in. (1.2 to 2.5 cm). Photograph by Samuel V. Panno; used by permission.

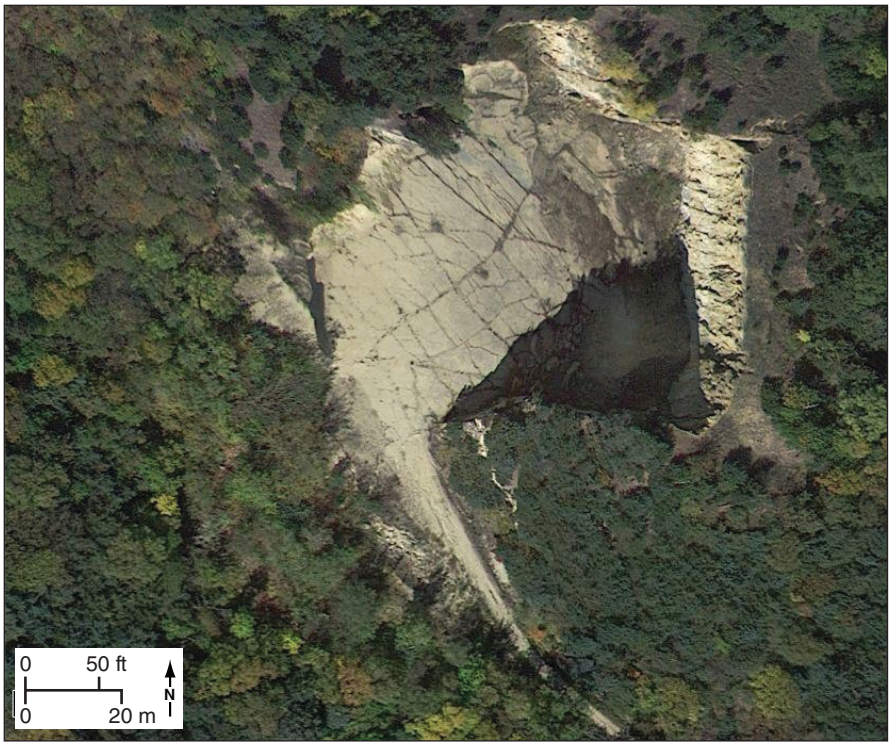

Figure 31 Aerial photograph of the Crawford Quarry (Map 1) showing a fracture–crevice pattern in the quarry floor that is enhanced by vegetation. Photograph © Google (December 2015).

Miner Road Quarry

The Miner Road Quarry is located about 3 mi (5 km) due east of Galena and contains abundant near-vertical fractures, solution-enlarged crevices and bedding planes, and at least one cave. The height of the quarry walls ranges from 30 to 65 ft (10 to 20 m), and the exposure reveals the nature and extent of the porosity of the Galena Dolomite with depth. Crevice widths range from 0.4 in. to 1 ft (1 cm to 0.3 m); the cave opening is about 5 ft (1.5 m) in diameter (Figure 33a,b).

Recharge to and Groundwater Flow Within the Galena Dolomite

It is possible to use exposures of fractures and crevices in road cuts and quarry walls as an example of fracture and crevice morphology in the Galena Dolomite. On the basis of their length, width, and distribution, these fractures and crevices are abundant and responsible for the vegetative crop lines in the Driftless Area associated with thin soils overlying the Galena Dolomite (Panno et al. 2015). From road cut and quarry exposures, it is obvious that most of the crevices are filled with fine-grained sediment near the surface that would slow infiltration into the bedrock aquifer. Because of these infillings, it was not clear how recharge and rapid movement through the aquifer would occur. A detailed examination of the fractures and crevices exposed within the quarries and road cuts provided a better understanding of the function and behavior of these features in three-dimensional space. Typically, crevices at the soil–bedrock interface are filled with fine-grained sediment, probably from the soil zone, whereas smaller aperture fractures contain little, if any, sediment. In addition, deeply penetrating roots from trees and other larger forms of vegetation tend to follow crevices. Both fracture openings and root paths through sediments trapped within crevices should provide abundant pathways for recharge to the underlying aquifer. The occurrence of the

Figure 32 Numerous crevices oriented roughly east–west and ranging from tight fractures to more than 1 ft (30 cm) wide are common in the Good Miller Quarry located just south of Stockton, Illinois (Map 1). Photographs by Samuel V. Panno; used by permission.

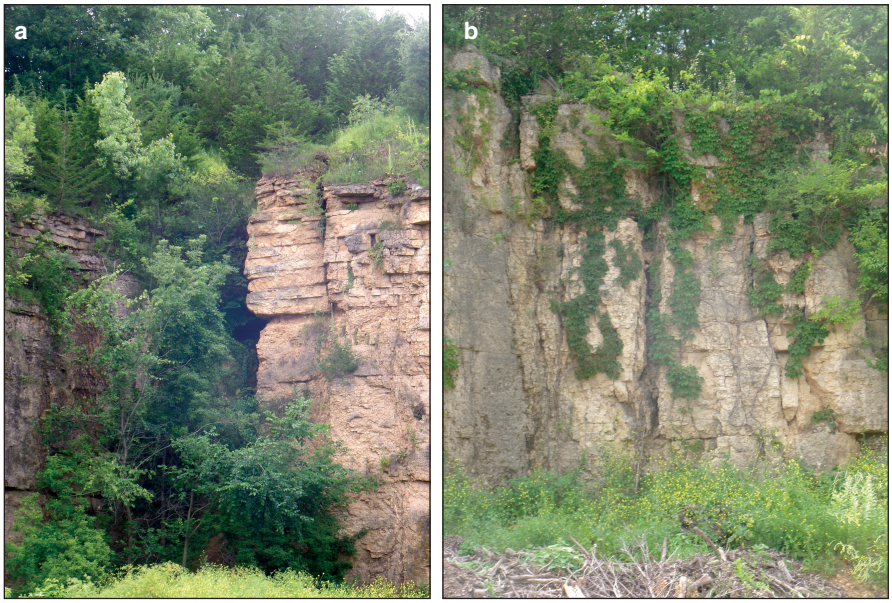

Figure 33 Crevice caves (a) and crevices and fractures (a, b) are common within the Galena Dolomite at the Miner Road Quarry (Map 1). Bedding planes are also visible, and many are solution enlarged, allowing for groundwater movement. Photographs by Samuel V. Panno; used by permission.

sediment-free crevices near the base of the Good Miller Quarry floor (Figure 32) and sediment-free crevices within the Miner Road Quarry (Figure 33) suggests that open crevices occur at a depth of about 50 ft (15 m) in both Silurian dolomite and Galena Dolomite. These open crevices would provide the opportunity for recharge flowing through fractures and along root paths within crevices to converge into underlying open crevices, which could serve as collector conduits where the more rapid groundwater flow is likely to occur. That rapid flow of groundwater through open conduits is classic karst behavior of an aquifer. In areas where crevices are open at the surface, landowners have reported sinkholes and localized rapid recharge in the Driftless Area of Illinois.

Hydrologic Features

Springs

Open crevices and bedding plane partings are also observed within the Galena Dolomite, where numerous springs (discussed below) discharge at the surface (Figure 34a,b). Springs are common features throughout Jo Daviess County, and Reed (2008) and Maas (2010) have mapped the locations of some. At present, the only available data on the chemical composition of springs in the county are from Maas (2010) for six springs in northeastern Jo Daviess County within the Warren Quadrangle (Map 1). However, the first three authors of this circular are presently sampling more than 30 springs in Jo Daviess County. The springs are consistent with the discharge of groundwater along bedrock crevices and bedding planes, where the overburden thins near stream valleys. Groundwater, under hydrostatic pressure, would be able to breach land surface in low-lying areas with relatively thin overburden (usually near streams). Bedrock springs are of two types. The first type appears as relatively small, solution-enlarged bedding planes (Figure 34a) from which relatively small volumes of groundwater discharge. The second type has the greater discharge, and they appear as large circular to elliptical depressions (Figure 34b) with a small section of the circular depressions breached, providing openings through which the groundwater discharges, creating a small tributary.

Chemical Composition of Groundwater

Data used to characterize the chemical composition of groundwater within the shallow Galena Dolomite aquifer were collected from 10 wells and one spring by the authors (Table 2) and by Maas (2009). Maas (2010) collected monthly samples from six springs discharging from Galena Dolomite in northeastern Jo Daviess County from spring to fall of 2009. The springs were named after the owners and include Hicks, Heller, Cora,

Figure 34 Springs within the Galena Dolomite in Jo Daviess County discharge at rates of <1 to 10 L/s (Map 1). The smaller spring (a) is discharging from a 0.4-in. (1-cm)-wide bedding plane. The larger springs (b) appeared to be discharging from an open crevice and associated fractures. The tubular instrument measuring field parameters in both photographs is a Hydrolab and is about 3 in. (8 cm) wide and 2 ft (60 cm) in length. Photographs by Samuel V. Panno; used by permission.

Sargent, McPhillips, and Holesinger Springs (Map 1). Because spring water in karst regions is an amalgam of groundwater from various sources and ages, the chemical composition of spring water is useful in characterizing background concentration ranges of constituents and trends in surface-borne contaminants (Table 1). The overall chemical composition of groundwater and the relationships between and among selected cations and anions were used to identify the source(s) of contaminants in Jo Daviess County aquifers. Background concentration ranges of selected ions are useful for comparing natural compositions of surface water and groundwater with water sources that have been affected by anthropogenic or natural contaminants, or both. When making such comparisons, one must be aware that, for example, concentrations of sodium (Na), chloride (Cl^-) and nitrate-nitrogen (NO_3-N) that are somewhat elevated above background generally do not constitute water that is harmful to humans or to the natural flora and fauna of an area. Elevated concentrations do, however, indicate that surface-borne contaminants from land-use activities have entered the aquifer and will ultimately discharge to surface waters. Further, it has been shown that elevated concentrations of Na and Cl^- can be deleterious to vegetation (e.g., Panno et al. 1999) and aquatic organisms (e.g., Kelly et al. 2012), can impart a salty taste to drinking water at concentrations exceeding 250 mg/L, and, for elevated Na concentrations in drinking water, may be a problem for people with high blood pressure (USEPA 2014). Nitrate-N concentrations >10 mg/L in drinking water have been shown to cause methemoglobinemia (blue-baby syndrome) and may be linked to stomach cancer (O'Riordan and Bentham 1993). For the purposes of this investigation, we considered concentrations exceeding the upper end of background as anthropogenic tracers that may be used to investigate aquifer recharge areas, recharge rates, and groundwater movement within the underlying karst aquifer.

Groundwater in Jo Daviess County is a Ca-Mg-bicarbonate (Ca-Mg-HCO_3^-)-type water with elevated concentrations of Cl^- and NO_3-N in some areas (Panno and Luman 2008). Hardness values (defined as Ca × 2.5 + Mg × 4.1) for well water range from 303 to 494 mg/L (Table 2); values greater than 180 mg/L are considered very hard. The background concentration range for Cl^- in shallow groundwater in northern and central Illinois is between 1 and 15 mg/L (Panno et al. 2006a). The range for background concentration of NO_3-N in Illinois is between 0 and 2.5 mg/L (Panno et al. 2006b; Hwang et al. 2015). Potential sources of Cl^- and NO_3-N include road salt, human and animal waste, and fertilizers. On the basis of chemical compositions of groundwater from wells and springs, the distribution of these ions and relatively high DO concentrations in the underlying aquifer are indicative of an open, oxygenated, unconfined karst system. Median DO concentrations from Mass (2010) for six springs were 0.96, 5.38, 6.21, 6.34, 6.57, and 6.84 mg/L. All but one, Hicks Spring (Map 1), contained DO levels near what would be expected in surface water. Dissolved oxygen in shallow wells (70 to 160 ft [21 to 49 m]) were lower, ranging from 3.5 to <0.1 mg/L. Water resources in open aquifer systems such as this are especially vulnerable to surface-borne contaminants.

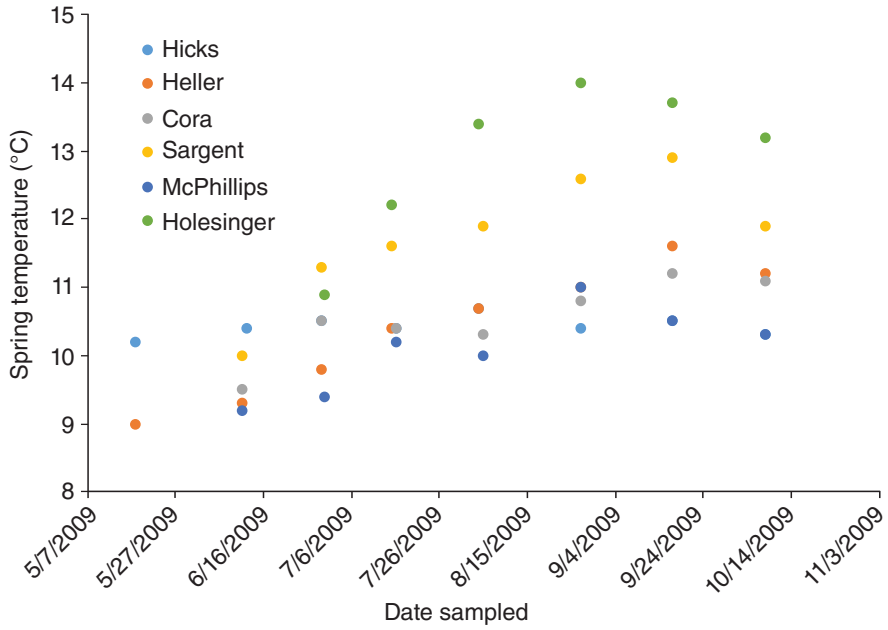

Figure 35 Spring temperature versus time showing the variability of seasonal spring-water temperatures. Those springs with the greatest variability are probably more open systems, that is, groundwater flow systems that are flowing through larger aperture crevices and conduits. Data from Maas (2010).

There is little or no attenuation of contaminants discharged into sinkholes, macropores, and fissures; consequently, wells, springs, and streams downgradient of contamination sources can show effects within a few days or even hours (Green et al. 2006). The convergent nature of flow in karst aquifers may result in contaminants becoming concentrated in conduits (Field 1993).

Data from Maas (2010) and Maas and Peterson (2010) in the eastern part of Jo Daviess County indicated that water from five of the six springs discharged from open, oxygenated systems and typically contained Cl^- (5.44 to 26.7 mg/L) and NO_3-N (2.92 to 30.1 mg/L) concentrations above background (Map 1). Spring water from all six springs was undersaturated with respect to calcite and dolomite. The lack of saturation with respect to the common carbonate minerals calcite and dolomite indicates that recharge to these springs was relatively recent and that karstification of the Galena Dolomite is an ongoing process in this area. The elevated concentrations of NO_3-N found in all but one of the springs are similar to those found in tile drain waters in Illinois. Tile drains have been described by Schilling and Helmers (2008b) as analogous to karst drainage basins with regard to nutrient losses in an agricultural watershed. The elevated nutrient concentrations in the springs suggest that the springs studied by Maas (2010) may be affected by recharge water containing relatively high concentrations of surface-borne contaminants. The relative depths of the groundwater flow system feeding the springs may be estimated by the changes in temperature of the spring water with time (Figure 35). Specifically, the shallowest flow systems would be most affected by seasonal changes that would manifest in the fluctuation of spring-water temperatures. All but Hicks Spring (Map 1) were affected by seasonal changes, and Holesinger Spring was the most affected (Figure 35).

Because of the nature of groundwater flow in karst aquifers, groundwater pathways may be discrete conduits or crevices, bedding planes, or both and may be fed by numerous smaller crevices within the carbonate bedrock. Because springs are discharge points for groundwater, they may be fed by numerous flow paths of various ages. Some of the input may have a shallow component containing surface-borne contaminants from a variety of land uses, whereas other inputs may originate from deeper, usually less contaminated, sources. The percentages of each component source can vary depending on the groundwater flow paths to the springs and can vary with time or season.

Background concentrations of major ions and contaminants are presented in Table 1. Most of these concentrations were determined by Panno et al. (2006a,b) from groundwater samples from the karst region of southwestern Illinois. We also inferred concentrations by using data from Hicks Spring (Map 1), which appeared to be less affected by recharge events and surface-borne contaminants than the other springs sampled by Maas (2010). Distinct differences can be seen among the six springs sampled by Maas (2010) based on concentrations of indicators of surface-borne contamination, which include potassium (K), Na, Cl, and NO_3-N. Maas (2010) concluded that concentrations of Cl^-, NO_3-N, Na, and sulfate (SO_4^{2-}) were anomalous and were derived from

Table 1 Range of concentrations and estimated background threshold values for parameters and ions determined from spring-water samples collected by Maas (2010) in eastern Jo Daviess County[1]

Parameter	Range	Background threshold
pH	6.35–6.90	ND
Specific conductance (µS/cm)	520–1,100	700**
Ion (mg/L)		
Sodium (Na)	5.7–13.4	10.0 m/L**
Potassium (K)	0.21–3.76	1.2 m/L**
Calcium (Ca)	62.2–105	ND
Magnesium (Mg)	35.8–56.6	ND
Silicon (Si)	4.5–8.0	ND
Bicarbonate (HCO_3)	175–400	ND
Chloride (Cl^-)	1.1–26.7	15.0 m/L*
Fluoride (F^-)	0.08–0.38	0.4 m/L**
Sulfate (SO_4^{2-})	8.32–31.1	35.0 m/L**
Nitrate-nitrogen (NO_3-N)	<0.3–30.1	2.5 m/L*

[1]Threshold values are the upper bounds of background concentrations and were estimated based on previous work by Panno et al. (2006a,b)*, unpublished data are from the sinkhole plain of southwestern Illinois (S. Panno, ISGS), and spring data are from Hicks Spring** (Maas 2010) located in eastern Jo Daviess County. ND = not determined.

surface-borne contaminants. However, because the geology of Jo Daviess County is not limited to carbonate rock, other strata (e.g., shale) could have contributed Na and SO_4^{2-} to the groundwater. Potential contaminants in the area include fertilizers and road salt (NaCl). Fertilizers used in the area include urea, 28% solution N, anhydrous ammonia, diammonium phosphate, potash, and, on a local basis, hog and dairy manure. McPhillips Spring (Map 1) is near a dairy where manure is applied to the fields (J. Frances, Warren, Illinois, personal communication, June 2013). Because households in this area are on private septic systems, waste from septic effluent is also a possible source of these ions (Panno et al. 2007).

Preliminary work by Panno and Luman (2008) on water-quality data from public water supply wells in Jo Daviess and Stephenson Counties showed that Cl^- concentrations ranged from <1 to 55 mg/L and NO_3-N concentrations ranged from <0.1 to 31 mg/L. The municipal well data from Jo Daviess County suggested that elevated (above background) NO_3-N was found at depths of up to 210 ft (64 m), and elevated Cl^- was also found at depths of up to 210 ft (64 m). Well construction problems or erroneous data likely account for the NO_3-N and Cl^- anomalies below these depths (Figures 36 and 37). Denitrification probably accounts for the very low concentrations to absence of NO_3-N below 210 ft (64 m). Background concentrations in this area appear to be lower than the estimated 15 mg/L of Cl^- and 2.5 mg/L of NO_3-N (Table 1). Estimates for background concentrations of Cl^- and NO_3-N when using municipal well data are slightly lower, about 1 to 10 mg/L and <0.1 to 2 mg/L, respectively. The deeper groundwater in the area from wells that intersect the St. Peter Sandstone have Cl^- concentrations between <1 and 3 mg/L in Jo Daviess County and about 1 mg/L in the Galena area. Chloride concentrations in aquifers at that depth are anomalously low, given that the lowest Cl^- concentration in the aquifer (0.6 mg/L) is slightly above the concentration of Cl^- in rainwater (0.1 to 0.3 mg/L) and slightly less than that of soil water (0.7 to 1.7 mg/L; Panno et al. 2006a). Processes in the unsaturated zone (e.g., evapotranspiration) and rock–water interaction typically increase the Cl^- concentration of groundwater up to 15 mg/L. Recharge of glacial meltwater would be capable of leaching soils and bedrock aquifer flow paths to the extent that they would impart little Cl^- to the groundwater via rock–water interaction. This effect is apparent in part of the Mahomet aquifer in east central Illinois (Hackley et al. 2010).

The pH values of spring water sampled by Maas (2010) were always below 7.0, which are consistent with the spring water being undersaturated with respect to calcite and dolomite. Water in equilibrium with calcite or dolomite would have pH values greater than 8.0. These lower pH values indicate that groundwater from the springs is not in equilibrium with carbonate rock, which supports the interpretation of an open karst system.

Specific conductance is a measurement of the electrical conductance of the water that can easily be measured in the field and is highly correlated with the amount of dissolved material in the water. The approximate background values in groundwater within the karst regions of southwestern Illinois and northwestern Illinois range from 650 and 700 µS/cm based on available data by Maas (2010), Panno (ISGS, unpublished data), and Hackley et al. (2007). We estimate a background value of 700 µS/cm for Jo Daviess County. This value should be considered preliminary, given the relatively small number of groundwater samples collected within the study area.

The Ca-Mg-HCO_3^--type water was expected because groundwater from each spring and well is discharging from the fractured and creviced Galena Dolomite aquifer. Groundwater in equilibrium with dolomite should have an alkaline pH value and a Mg/Ca weight ratio ranging from 0.471 to 0.623; pure dolomite dissolved by fresh water should have a Mg/Ca weight ratio of 0.61. Thus,

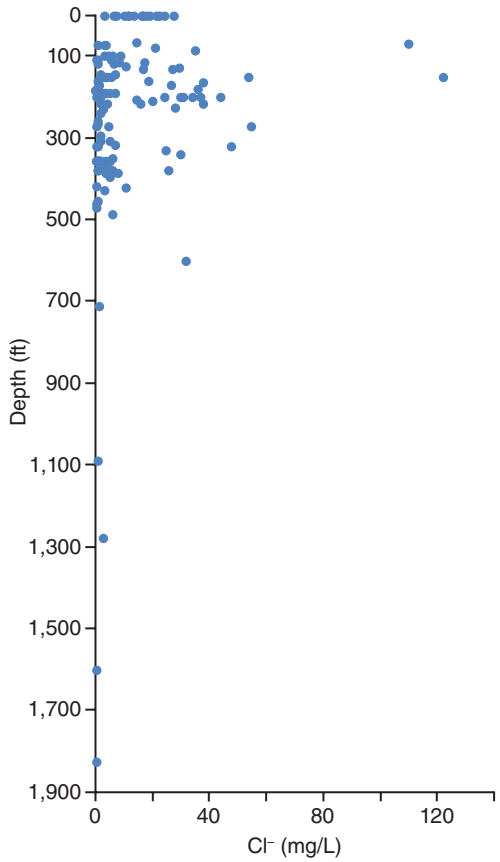

Figure 36 Cl^- (mg/L) versus depth (ft) in the Galena and Platteville Groups for municipal wells in Jo Daviess County. Cl^- concentrations are sporadically elevated above the natural background for groundwater to depths of up to 210 ft (64 m). This behavior is consistent with groundwater flow within a fractured and creviced aquifer.

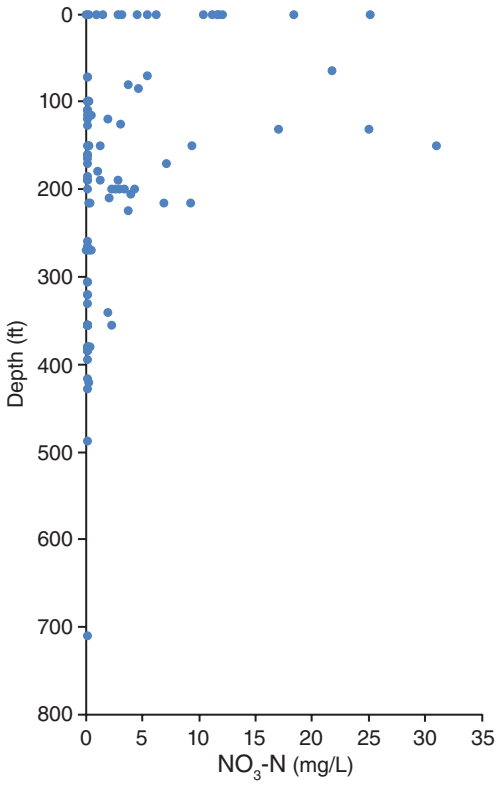

Figure 37 NO_3-N (mg/L) versus depth (ft) in the Galena and Platteville Groups for municipal wells in Jo Daviess County showing the greatest enrichment in the upper 150 ft (46 m). These concentrations are sporadic and elevated above the natural background for groundwater to depths of up to 210 ft (64 m). This behavior is consistent with groundwater flow within a fractured and creviced aquifer.

most of the samples are consistent with dissolution of dolomite (all but one range from 0.516 to 0.623). The sample with the lowest weight ratio of 0.417 may be affected by limestone facies present within the Galena Group (Willman et al. 1975). Samples in equilibrium with the host dolomite would lie close to the Ca/Mg 1:1 molar ratio line (Figure 38). Although we have no background values for Ca and Mg, it is likely that concentrations of these would be near the upper bounds of the ranges presented in Table 1. It is clear that in the groundwater from the aquifers we sampled, dolomite has not been dissolved to equilibrium. This is probably because of the influx of and mixing with recent recharge, which is

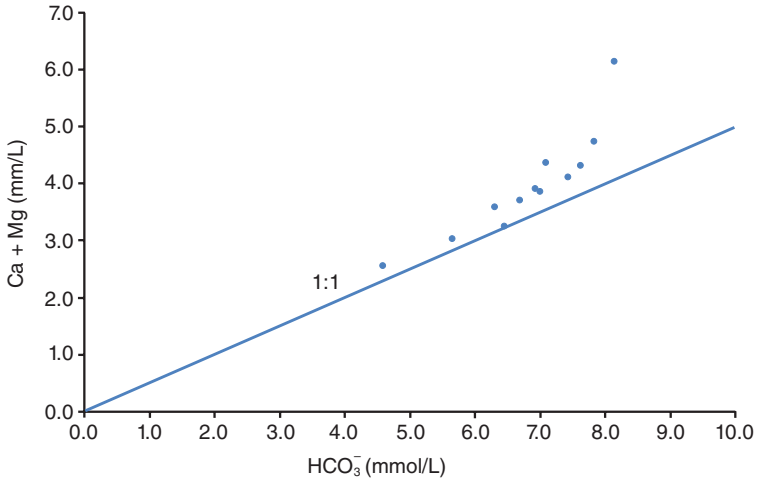

Figure 38 Ca plus Mg versus HCO_3^- (mmol/L) showing the effects of dissolution of dolomite, potentially mixed with the effects of the oxidation of pyrite. The 1:1 line represents molar ratios and not concentrations.

Table 2 Groundwater samples collected from 11 shallow wells and one spring from across Jo Daviess County in July 2014[1]

Site no.	Well depth (m)	Year drilled	Water source (formation)	Casing length (m)	Temp. (°C)	pH	SpC (µS/cm)
Well 1	33.5	1996	Platteville	19.5	11.5	6.64	567
Well 2	35.4	1991	Platteville	25.9	11.4	6.58	675
Well 3	38.1	2009	Grey ls.	25.0	11.7	6.65	663
Well 4	36.6	2010	Grey ls.	25.0	12.2	6.67	673
Well 5	48.8	ND	Galena	29.6	13.6	6.57	805
Well 6	33.5	2004	Galena	19.5	12.4	6.61	663
Well 7	33.5	2003	Galena	13.7	11.7	6.73	520
Well 8	35.0	2004	"Ls. with py"	26.8	17.9	6.67	664
Well 9	30.5	2006	Galena	25.9	11.7	6.63	743
Well 10	38.7	1994	Galena	30.5	11.7	6.56	773
G-well	21.3	ND	Galena	21.3	12.3	6.57	1,223
G-spring	ND	ND	ND	ND	13.3	7.02	366

Site no.	ORP (mV)	DO (mg/L)	Ba (mg/L)	Ca (mg/L)	Fe (mg/L)	K (mg/L)	Li (mg/L)
Well 1	163	<0.1	0.14	69.8	0.118	1.28	<0.11
Well 2	275	0.4	0.03	80.1	<0.024	1.14	<0.11
Well 3	333	3.5	0.05	74.1	<0.024	2.20	<0.11
Well 4	357	2.8	0.03	81.6	<0.024	0.85	<0.11
Well 5	323	0.1	0.05	101	<0.024	1.00	<0.11
Well 6	307	0.1	0.11	82.8	0.038	1.23	<0.11
Well 7	231	0.1	0.10	63.1	0.076	1.61	<0.11
Well 8	370	0.3	0.13	81.2	<0.024	1.10	<0.11
Well 9	258	<0.1	0.03	86.1	0.092	0.92	<0.11
Well 10	256	0.4	0.24	94.6	0.168	1.06	<0.11
G-well	439	5.9	0.008	131	0.024	1.88	<0.11
G-spring	175	0.2	0.13	50.3	0.161	2.31	<0.11

Site no.	Mg (mg/L)	Mn (mg/L)	Mo (mg/L)	Na (mg/L)	P (mg/L)	Pb (mg/L)	Sb (mg/L)
Well 1	36.9	0.01	<0.022	4.52	0.100	<0.041	<0.059
Well 2	45.3	0.00	<0.022	5.81	0.100	<0.041	<0.059
Well 3	45.5	<0.0015	<0.022	4.62	0.100	<0.041	<0.059
Well 4	50.8	<0.0015	<0.022	3.22	<0.073	<0.041	<0.059
Well 5	54.4	0.01	<0.022	5.64	<0.073	<0.041	<0.059
Well 6	45.1	0.00	<0.022	3.53	<0.073	<0.041	<0.059
Well 7	35.7	0.01	<0.022	2.08	0.100	<0.041	<0.059
Well 8	38.2	0.02	<0.022	7.68	0.120	<0.041	<0.059
Well 9	53.0	0.17	<0.022	5.74	0.120	<0.041	<0.059
Well 10	48.9	0.02	<0.022	10.3	<0.073	<0.041	<0.059
G-well	70.1	0.00	<0.022	53.4	<0.073	<0.041	<0.059
G-spring[2]	31.9	0.00	<0.022	1.37	<0.073	<0.041	<0.059

Site no.	Se (mg/L)	Si (mg/L)	Sn (mg/L)	Sr (mg/L)	Zn (mg/L)	Alkalinity (mg/L as CaCo)	F (mg/L)
Well 1	<0.13	6.00	<0.086	0.086	0.0490	322	0.294
Well 2	<0.13	5.79	<0.086	0.010	0.0330	350	0.116
Well 3	<0.13	5.68	<0.086	0.002	0.0390	334	0.088
Well 4	<0.13	6.49	<0.086	0.013	<0.0097	371	0.139
Well 5	<0.13	8.07	<0.086	0.054	0.0810	391	0.210
Well 6	<0.13	6.30	<0.086	0.048	0.0290	346	0.188
Well 7	<0.13	4.51	<0.086	0.054	<0.0097	282	0.217
Well 8	<0.13	6.40	<0.086	0.046	0.1700	315	0.236
Well 9	<0.13	7.35	<0.086	0.031	0.0190	381	0.158
Well 10	<0.13	8.23	<0.086	0.065	0.1180	354	0.177
G-well	<0.13	10.3	<0.086	0.181	0.0270	407	0.140
G-spring[2]	<0.13	8.75	<0.086	0.078	<0.0097	229	0.250

Continued on next page

Table 2 *Continued.*

Site no.	Cl (mg/L)	Br (mg/L)	NO_3-N (mg/L)	SO_4 (mg/L)	o-PO_4-P (mg/L)	NVOC (mg/L)	TKN (mg/L)
Well 1	0.68	<0.08	<0.04	7.79	0.012	0.320	<0.16
Well 2	8.65	<0.08	0.43	31.0	0.012	0.515	<0.16
Well 3	10.9	<0.08	3.07	22.4	0.018	0.397	<0.16
Well 4	6.55	<0.08	1.89	17.0	0.013	0.333	<0.16
Well 5	18.6	<0.08	<0.04	51.3	0.017	<0.310	<0.16
Well 6	5.66	<0.08	<0.04	33.1	0.013	<0.310	<0.16
Well 7	1.14	<0.08	<0.04	16.3	0.010	0.386	<0.16
Well 8	17.4	<0.08	<0.04	37.3	0.012	0.483	<0.16
Well 9	9.02	<0.08	0.19	42.1	0.015	<0.310	<0.16
Well 10	29.7	<0.08	<0.04	49.3	0.017	0.453	<0.16
G-well	110	<0.08	5.42	104	<0.073	ND	ND
G-spring[2]	1.10	<0.08	<0.04	17.9	<0.073	<0.280	ND

Site no.	NH_3-N (mg/L)	Total coliforms	*E. coli*	δD_{H2O} (‰)	$\delta^{18}O_{H2O}$ (‰)	Tritium (TU)
Well 1	0.06	Present	Absent	–48.2	–7.63	0.60
Well 2	<0.03	Present	Absent	–56.3	–8.61	3.25
Well 3	<0.03	Absent	Absent	–54.2	–8.39	5.45
Well 4	<0.03	Absent	Absent	–53.3	–8.24	4.11
Well 5	<0.03	Absent	Absent	–53.7	–8.33	4.34
Well 6	<0.03	Present	Absent	–52.7	–8.23	1.71
Well 7	<0.03	Absent	Absent	–56.4	–8.45	0.60
Well 8	<0.03	Absent	Absent	–54.6	–8.38	2.28
Well 9	<0.03	Absent	Absent	–56.0	–8.62	3.41
Well 10	<0.03	Absent	Absent	–54.5	–8.52	3.42
G-well	ND	Absent	Absent	–53.5	–8.02	4.92
G-spring[2]	<0.03	Present	Present	–50.2	–7.50	0.64

[1]SpC, specific conductance; ND, not determined; G-spring, Galena Trail Spring (Map 1); ORP, oxidation–reduction potential; DO, dissolved oxygen; ls., limestone; ls. with py, limestone with pyrite; NO_3-N, nitrate nitrogen; o-PO_4-P, ortrophosphate-phosphorus; NVOC, nonvolatile organic carbon; TKN, total Kjeldahl nitrogen; NH_3-N, ammoniacal nitrogen; δD_{H2O}, delta deuterium of water; $\delta^{18}O_{H2O}$, delta oxygen-18 of water; TU, tritium units.

[2]Given the behavior of the field parameters of G-Spring over a period of one year (i.e., temperature, pH, and discharge remained constant), it is likely an unsealed well.

evident in the tritium data indicating the presence of modern water (Table 2). Samples in equilibrium with the host dolomite would lie close to the Ca/Mg 1:1 molar ratio line.

Potassium and Cl^- concentrations in spring water suggest that Holesinger Spring and, to a lesser extent, McPhillips Spring (Map 1) may be contaminated with potash fertilizer, manure, human waste, and road salt. Most of the groundwater samples from springs sampled by Maas (2010) exceed background concentrations for both ions. Only one sample (from Sargent's Spring, Map 1) falls on the K/Cl 1:1 molar ratio line. This particular sample experienced a 3- to 4-fold dilution (based on Cl^- concentrations) and a 10-fold or more increase in K after a recharge event in August 2009. Similar effects were seen in tile drain-fed stream-water samples from the same area during the same period (Maas 2010). Groundwater samples from McPhillips Spring (Map 1) contain slightly elevated concentrations of K and Cl^-, suggesting contamination by the aforementioned sources and likely by mixed sources. Groundwater samples from the other springs all fall below the K background threshold of 1.2 mg/L and may be affected by sources dominated by NaCl, such as water softeners and road salt (e.g., Panno et al. 2006a; Table 1, Figure 39). This estimated background for K is slightly greater than that found in the karst springs of southwestern Illinois' sinkhole plain, of <1 mg/L (S. Panno, ISGS, unpublished data).

Nitrate-N concentrations for most of the springs were greater than those in most shallow groundwater in Illinois (Figure 40) and far exceeded the background value of 2.5 mg/L (Table 1). Nitrate-N concentrations ranged between 11 and 30 mg/L (median of 12.3 mg/L) for five of the six springs and exceeded concentrations found in tile drains of central Illinois measured by the authors (e.g., ranging from 0.51 to 23.1 mg/L, median of 11.3 mg/L; Panno et al. 2005) and in tile drain-fed surface streams in Jo Daviess County (i.e., ranging from 4.19 to 14.6 mg/L, median of 9.31 mg/L; Maas 2010). This result is not surprising, given that row crop agriculture is the dominant land use in the area and that N fertilizer and manure are commonly applied to the fields. However, the NO_3-N concentrations were surprisingly constant over time for Heller and Cora Springs (Map 1) and showed few, if any, seasonal effects; the median concentration was about 12 mg/L. Only McPhillips and Holesinger

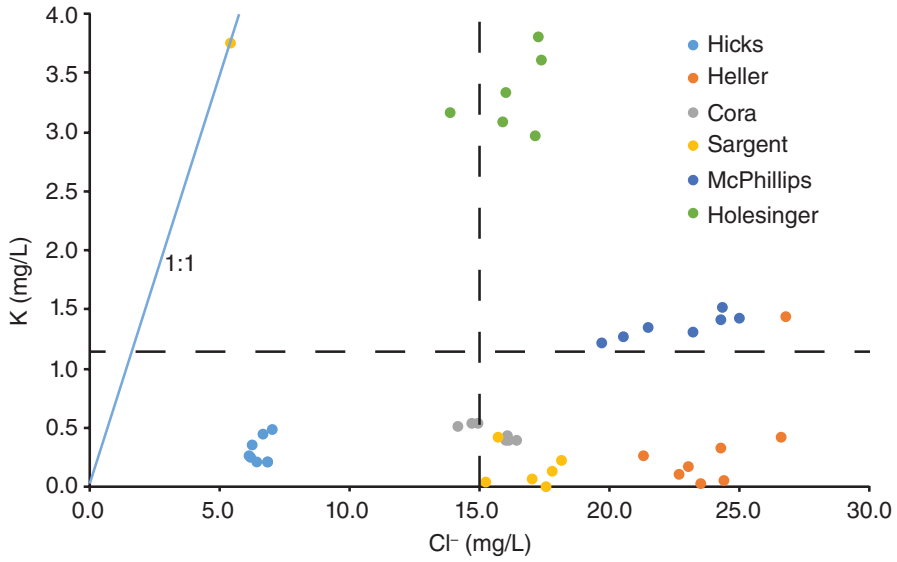

Figure 39 K versus Cl^- (mg/L) showing spring-water samples relative to background concentrations of each ion (dashed lines). Data from Maas (2010). The 1:1 line represents molar ratios and not concentrations.

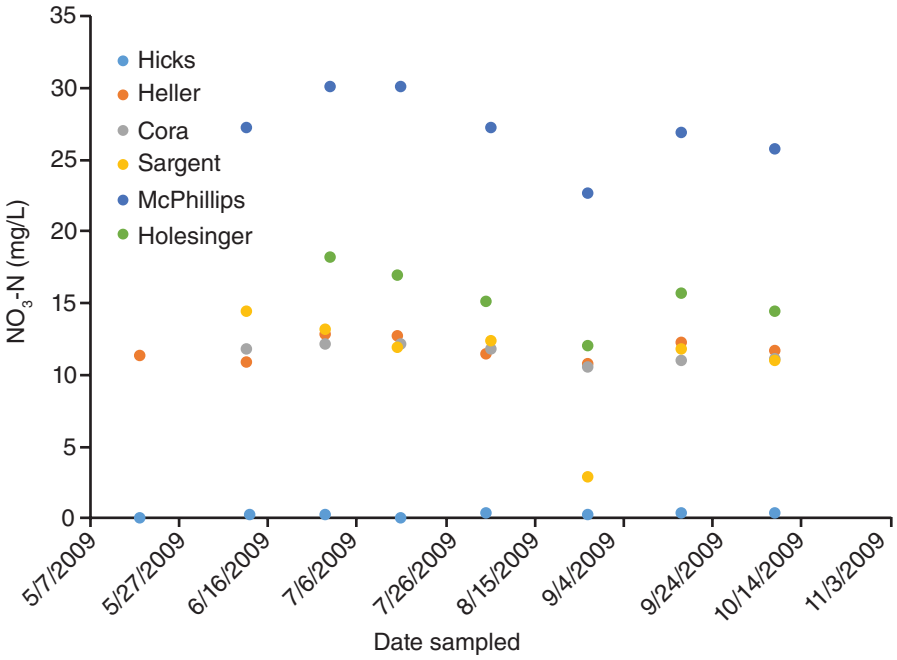

Figure 40 NO_3-N (mg/L) versus time showing the effects of surface-borne contamination on the six springs. Hicks Spring is least affected (if at all), and McPhillips Spring is most affected. Sargent's Spring appears to be most affected by a recharge event during the summer of August 2009. Data from Maas (2010).

Springs (Map 1) showed seasonal effects. They also had the greatest concentrations of NO_3-N and median concentrations of 27 and 16 mg/L, respectively, with some dilution in samples collected in August 2009. Nitrate-N concentrations in Hicks Spring (Map 1) were very low, what Panno et al. (2006b) determined to be indicative of the lower end of present-day background conditions (<0.4 to 2.5 mg/L). Although the low NO_3-N concentration in Hicks Spring (Map 1) samples could possibly be the result of denitrification, the background-level concentrations of Cl^- and K suggest that Hicks Spring (Map 1) more likely represents background concentrations for shallow groundwater in the area. Among the six springs sampled by Maas (2010), Hicks Spring (Map 1) appears to be the least affected by anthropogenic sources and recharge events.

All springs are in close proximity to land supporting row-crop agriculture, and one, McPhillips Spring (Map 1), is in close proximity to a livestock operation. However, the actual recharge areas of the springs are not known. Consequently, it is not possible at this time to use land use as an indicator of the sources of surface-borne contaminants in any more than a general way. Chloride and NO_3-N concentrations in Hicks Spring (Map 1) are well below background thresholds (15 and 2.5 mg/L, respectively; Figure 41). Because background concentrations for Cl^- and NO_3-N are exceeded in five of the six springs and because the ions covary (Figure 41), the data suggest that these springs are being fed by an aquifer with a steady input of these ions. The data also suggest that the ions are entering the aquifer together, perhaps as manure, septic effluent, or both. A plot of Na versus Cl^- for all the spring data shows no discernible relationship, indicating that road salt is either not the likely source of either ion in the springs or, more likely, the degree of ion exchange is not uniformly represented in the springs.

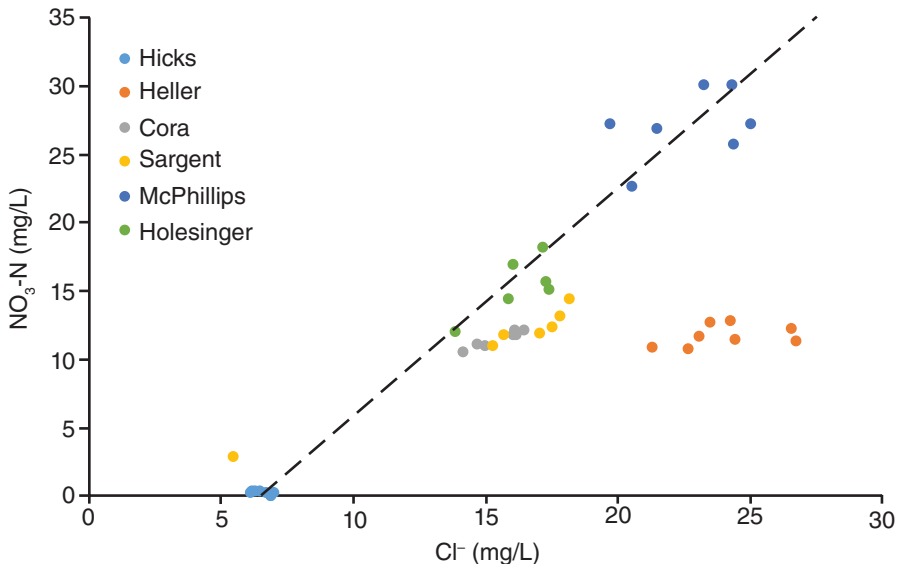

Figure 41 Cl^- versus NO_3-N (mg/L) for spring-water samples. All but Hicks Spring are above the background for both ions, and all but Heller Spring data plot along a trend line (dashed line) that may be related to the application of manure and N fertilizer on croplands. Data from Maas (2010).

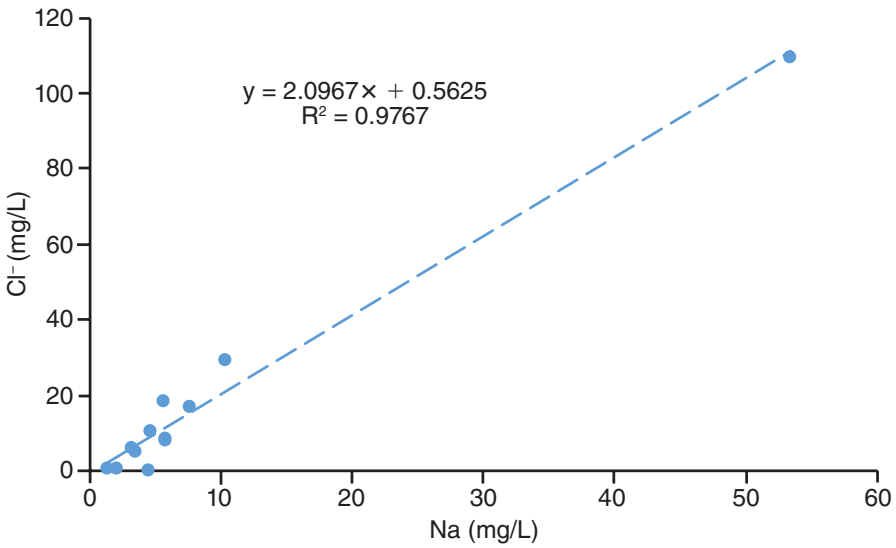

Figure 42 Na versus Cl^- (mg/L) showing a strong correlation between the two ions. This result suggests that anthropogenic contaminants (e.g., road salt, septic effluent) contribute to the recharge areas of these springs. Data from Maas (2010).

Overall, the degree of contamination of the spring water with regard to NO_3-N is greater than that typically found in shallow groundwater of Illinois. This and the fact that concentrations of K and Cl^- exceed background concentrations in all but Hicks Spring indicate that N-based fertilizers, manure, human wastes, or their combination are likely entering the groundwater systems. The high DO concentrations in the spring samples (Maas 2010) suggest rapid movement of water into the subsurface, which would limit attenuation within the soil zone. In situations in which water recharges more slowly through the soil zone, oxygen is consumed as organic matter is reduced, resulting in anoxic conditions that promote denitrification, which would decrease NO_3-N concentrations. The thin soils and the presence of macropores and sinkholes in this area appear to promote rapid recharge to bedrock aquifers, a common feature of karst regions.

A preliminary investigation into the groundwater quality of the Galena Dolomite involved sampling 11 wells across Jo Daviess County (Map 1). To our knowledge, this is the first time wells in the Driftless Area of Illinois have been sampled on a systematic basis. The wells ranged from 70 to 160 ft (21 to 49 m) in depth. As with the spring-water samples, groundwater from all wells is a Ca-Mg-HCO_3^--type water with pH values ranging from 6.56 to 6.73. Tritium in groundwater samples from 10 of the wells ranged from 0.60 to 5.45 TU (Table 2), indicating that all well-water samples contained at least some component of modern recharge.

Evidence of modern recharge was also present for our well samples as surface-borne contaminants such as Na and Cl^- from road salt and septic effluent (Figure 42), NO_3-N from N-based fertilizers, manure and septic effluent, and bacterial indicators from septic effluent and manure. Tritium does not covary with depth, nor does it covary with Na or Cl^-. This lack of correlation may be a reflection of the highly fractured and creviced nature of the Galena Dolomite aquifer and the vagaries of well drilling. Available data from wells screened within the deeper Platteville Group and St. Peter Sandstone show anomalously low concentrations of Cl^- (about 1 mg/L). This result suggests that the upper part of the Galena Dolomite aquifer is most affected by surface-borne contaminants and that Cl^- is stratified throughout the carbonate aquifers, with anomalously low concentrations at depth (Figure 36).

Nitrate-N concentrations ranged from below the detection limit (<0.04 mg/L) to 5.42 mg/L; only two of the wells had NO_3-N concentrations that exceeded the background threshold concentration of 2.5 mg/L. Nitrate concentrations in the well samples correlated well with tritium concentrations; NO_3-N concentrations dropped below the detection limits (<0.04 mg/L) at about 3 TU

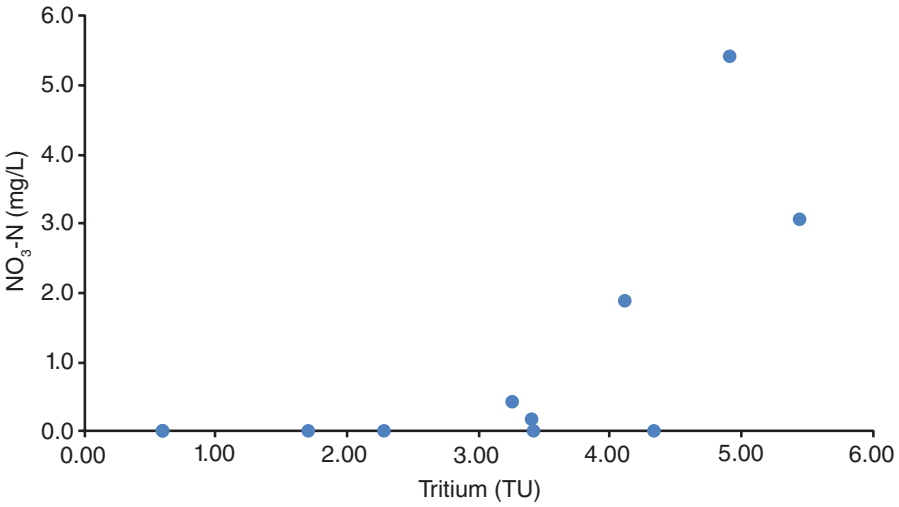

Figure 43 NO_3-N (mg/L) versus tritium (TU) showing an increase in NO_3-N concentrations with an increase in tritium concentrations. Nitrate concentrations decrease with time within the karst aquifer, probably because of denitrification (e.g., see Panno et al. 2001).

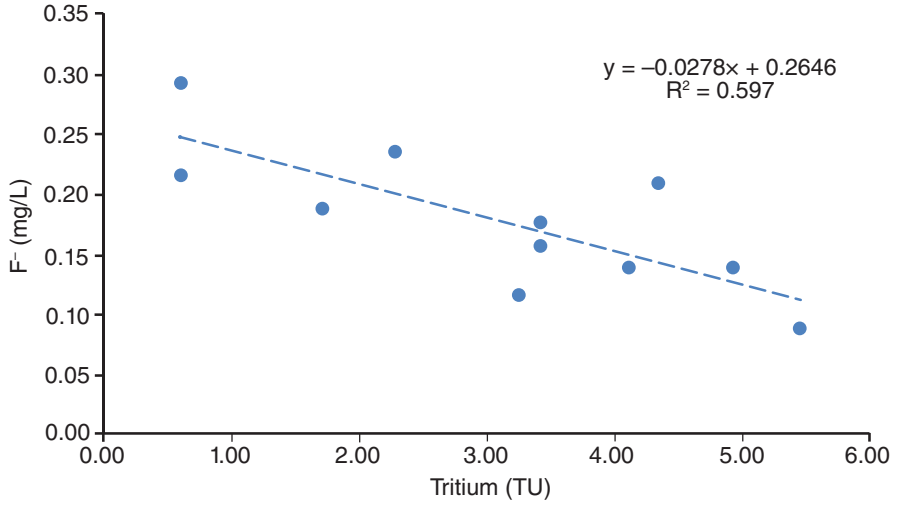

Figure 44 F^- (mg/L) and tritium (TU) covary, albeit with limited data, suggesting that F^- increases in concentration with time within the karst aquifer, probably because of rock–water interaction.

(Figure 43). This correlation may be the result of denitrification or mixing with tritium and NO_3-free groundwater from a deeper source, or both. However, the lack of correlation of Cl^- with tritium (Table 2) indicates that the latter mechanism (dilution) is not an important factor.

Tritium data for composite samples of rainwater collected in southwestern Illinois between 1999 and 2001 (n = 17) ranged from about 3 to 9 TU. A long-term estimate of tritium behavior with time suggests that the current concentrations of tritium in precipitation in North America (for roughly the last 10 years) should range from 3 to 5 TU (S.E. Effert-Fanta, ISGS, personal communication, 2015). Given that our shallowest well (21 m deep) had a tritium concentration of 4.92 (Table 2) and recent spring-water samples from Jo Daviess County had tritium concentrations ranging from 3.46 to 5.84 TU (all with evidence of rapid recharge (S. Panno [ISGS] and W. Kelly [ISWS], unpublished data), a range of 3 to 5 TU as the current background is reasonable. If this estimate is correct, NO_3-N appears to be absent after about one half-life, or 12.3 years. In any case, Figure 43 suggests that NO_3-N is actively being denitrified within at least the shallow Galena Dolomite aquifer.

Fluoride (F^-) appears to covary with tritium, increasing with the age of groundwater from about 0.1 mg/L for younger groundwater up to 0.30 mg/L for older groundwater (Figure 44). This suggests that F^- is derived from rock–water interaction and might serve as a surrogate or proxy for tritium in this area. However, only 11 data points make up this trend, and more data are needed to develop a statistically significant relationship between these parameters. Haamer and Karro (2006) and Uppin and Karro (2012) examined F^- anomalies in Silurian and Ordovician carbonate aquifers in Estonia and found that K-bentonite beds present within these aquifers (also present in Ordovician Dolomite in Jo Daviess County) are enriched in fluorine (F; 2,800 to 4,500 mg/kg) relative to the carbonate rocks (100 to 400 mg/kg). They found that 4 to 10 mg/kg of F could be leached from carbonate rocks, whereas 25 to 51 mg/kg of F could be leached from K-bentonites. Consequently, the F^-–tritium relationship (Figure 44) is consistent with rock–water interaction within Ordovician strata.

Calcium and SO_4^{2-} concentrations covary within shallow groundwater (Figure 45). Because of the abundance of pyrite and other sulfides within the Galena Dolomite (ore mineralization is ubiquitous throughout the county, as discussed earlier), the oxidation of pyrite (FeS_2) is likely the main source of SO_4^{2-} in the aquifer. Given the abundance of pyrite and other sulfides within the Galena Dolomite, the linear nature of the data, and their high degree of correlation, the sulfate is probably the result of the oxidation of pyrite present within the dolomite. That is, the oxidation of pyrite would result in the dissolution of dolomite [$CaMg(CO^3)_2$] and the precipitation of iron oxyhydroxide [$Fe(OH)_3$]. However, without supporting data, such as isotopic analyses of SO_4^{2-}, an evaporite

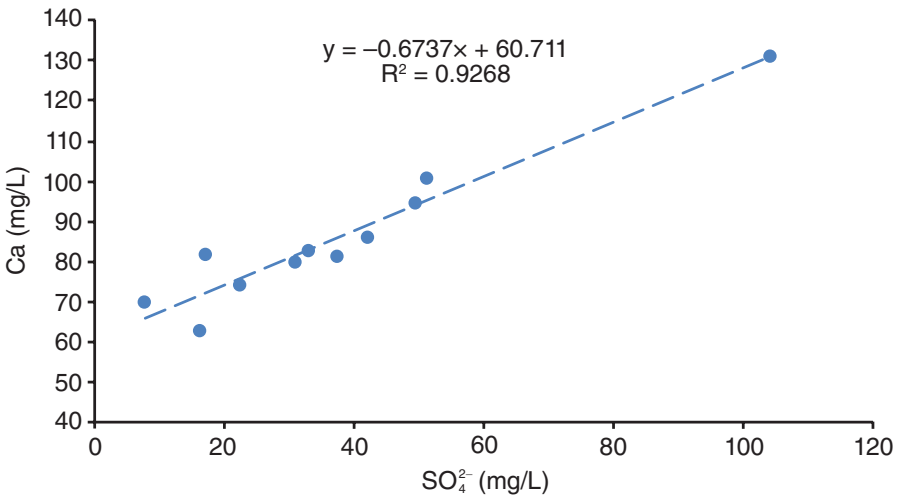

Figure 45 SO_4^{2-} versus Ca (mg/L) in shallow wells reveals a linear relationship that is common in groundwater. The linear relationship suggests a single source for the sulfate (i.e., the oxidation of pyrite).

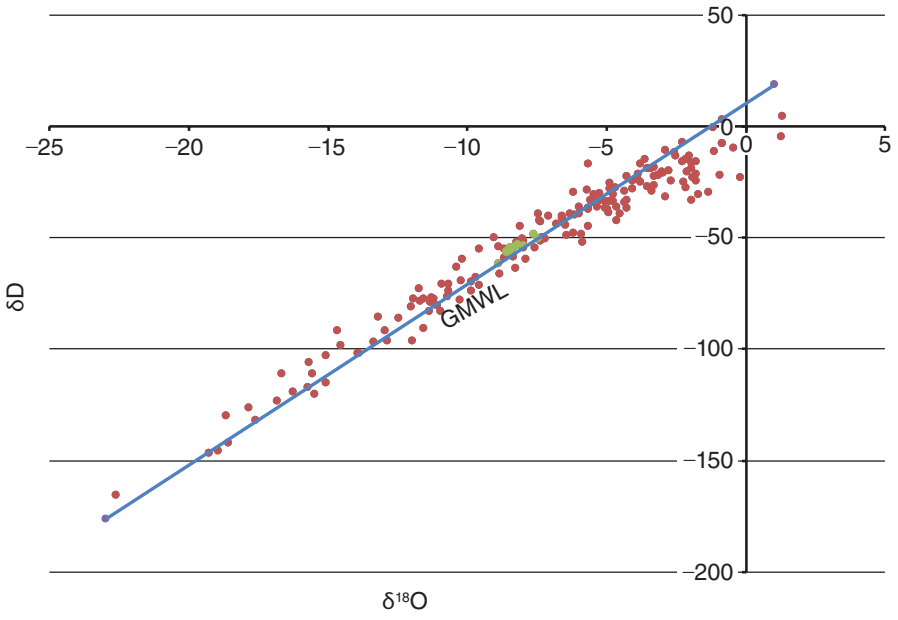

Figure 46 δD versus $\delta^{18}O$ for precipitation in Chicago, Illinois (Chicago Midway International Airport), from January 1960 through December 1979 (red; International Atomic Energy Agency 2015), and 12 tightly clustered groundwater samples collected from Jo Daviess County (green). The blue Global Meteoric Water Line (GMWL) is from Craig (1961).

source from a nearby state (e.g., Richardson and Hansen 1991) cannot be ruled out.

Data on δD and $\delta^{18}O$ from precipitation in Jo Daviess County should be similar to that of precipitation in the Chicago area, given that they share the same latitude and are only 150 mi (240 km) apart. Precipitation samples were collected in Chicago from 1960 through 1979 (International Atomic Energy Agency 2015). The Chicago data provide a local meteoric water line similar to that of the Global Meteoric Water Line. The stable isotope data for the groundwater samples collected in Jo Daviess County fall along this line (Figure 46) and indicate that little has occurred to recharge (e.g., evaporation) since entering the Galena Dolomite aquifer. Because the samples fall about midway within the range of precipitation data, the water samples are probably a mix of seasonal inputs with no input of older Pleistocene meltwaters.

Combining the water quality data we collected with those from the ISWS database yielded a representation of the vertical distribution of selected ions. The vertical distribution of surface-borne contaminants such as Cl^- and NO_3-N is distinctive (Figures 36 and 37). It is likely that elevated Cl^- concentrations are due to road salt contamination, septic effluent, and manure; however, the percentage of input from each is unknown. The highest Cl^- and NO_3-N concentrations are generally found in wells less than 210 ft (63 m) deep. This is the approximate depth at which the Galena Dolomite becomes shaley (Willman et al. 1975); shale would tend to limit the infiltration of contaminants at this depth. However, elevated Cl^- concentrations are sporadically found at depths greater than 210 ft (63 m) and may be due to questionable historic data, poor well construction, or fractures extending through the shale-rich strata (Figure 36). The vertical distribution of surface-borne contaminants is consistent with that of a fractured and creviced karst aquifer. Elevated NO_3-N concentrations are probably due to the application of N fertilizers in the area, given that land use in Jo Daviess County is dominated by row-crop agriculture. The relatively large NO_3-N concentrations near the surface are typical of agricultural areas, but, as with the Cl^- concentrations, the sporadic nature of the profile is consistent with a fractured and creviced karst aquifer. Below 210 ft (64 m), Cl^- and NO_3-N concentrations are typically below background levels.

The stable isotopes of the groundwater samples ranged from −48.2‰ to −56.3‰ and −7.63‰ to −8.62 ‰ for δD and $\delta^{18}O$, respectively (Table 2), and fall well within the range of present-day precipitation for northern Illinois. No evidence of evaporation is seen in these data, suggesting rapid infiltration following rainfall and snow melt. Overall, the chemical and stable isotopic compositions of

relatively shallow groundwater from wells within the Galena Dolomite aquifer is consistent with that of the springs and reflects an open, fractured karst aquifer whose mineralogy is dominated by dolomite. In addition, stratification of surface-borne contaminants and the effects of the fractured and creviced aquifer are indicated by available data.

SUMMARY AND CONCLUSIONS

This investigation into the geology and hydrogeology of Jo Daviess County has shown that carbonate bedrock contains solution-enlarged crevices that range from about 0.4 in. (1 cm) to more than 3 ft (1 m) in width and solution-enlarged bedding planes that are typically 0.4 in. (1 cm) in width or greater. These karst features are abundant and rarely spaced more than 30 ft (10 m) apart in road cut and quarry exposures. Cover-collapse sinkholes in fine-grained sediments overlying Silurian dolomite and located in the western part of the county are the largest and deepest sinkholes in Jo Daviess County, having widths up to 60 to 100 ft (20 to 30 m) and depths up to 6 to 21 ft (2 to 7 m). Cover-collapse sinkholes overlying Galena Dolomite are rarely obvious because of the thinner soils and the degree of cultivation, which tend to obscure all but the very largest of sinkholes. However, vegetated crop lines identified by Panno et al. (2015) from aerial photography during the extreme drought of 2012 revealed linear features that served as proxies for fractures and crevices of the underlying karst aquifer. The visible lines were the same orientation as crevices and fractures observed in road cuts and quarries and showed even closer spacing for east–west-trending fractures and crevices. The vegetated crop lines and the fractures and crevices in road cuts and quarries revealed the degree and extent of solution-enlarged crevices and connectivity of the karst aquifer in Jo Daviess County, adjacent counties of Illinois, and southwestern Wisconsin. These features showed that east–west- and north–south-trending fractures and crevices constitute the greatest porosity for aquifers of the Galena and Platteville Groups. Ground-penetrating radar and bedrock exposures in road cuts and quarries have shown that solution-enlarged crevices extend well into bedrock and are open at depth. All these approaches have provided a three-dimensional representation of the karst in Jo Daviess County.

The Galena Dolomite aquifer possesses properties of a fracture- and crevice-dominated karst system in at least the upper 60 ft (18 m) of the formation, based on road-cut and quarry observations. Solution-enlarged crevices in Galena Dolomite and Silurian dolomite follow the cleft karren model (linear, open crevices that narrow, but not close, with depth), whereas Silurian dolomite blocks atop knobs and ridges can slide on top of the Maquoketa Shale, resulting in a pseudo trench karren model in which the trenches terminate at the top of the shale. As noted, most crevices observed within the unsaturated zone contain fine sediments that may inhibit rapid infiltration of recharge into the Galena Dolomite. However, field observations suggest that abundant fractures containing little or no sediment are responsible for relatively rapid and focused recharge to the karst aquifer throughout the county via fractures, along root paths within crevice fillings, and through open crevices. Deeper within the aquifer (50 ft [15 m]) or more below land surface), open fractures, crevices, and conduits provide a network of pathways through which infiltrating surface water and groundwater can flow rapidly. Recharge to the karst aquifer is probably less rapid where it is overlain by Maquoketa Shale. In those areas where Maquoketa Shale constitutes the bedrock surface, tile drains are used to lower the water table.

Historic and recent groundwater quality data from domestic wells and recent spring data from Jo Daviess County indicate that the carbonate-hosted aquifer contains anomalously elevated concentrations of Cl^-, NO_3-N, and K, probably from potash and N fertilizers, livestock or human waste, and road salt. These data suggest that stratification of surface-borne contaminants within the aquifer has occurred over time. Groundwater quality within the Galena Dolomite aquifer of Jo Daviess County, based on samples from spring and shallow well data, are consistent with an open karst aquifer whose mineralogy is dominated by dolomite. Water chemistry data indicate that surface-borne contaminants have reached depths of 210 ft (64 m) in aquifers of the Galena and Platteville Groups.

ACKNOWLEDGMENTS

The authors thank Matthew Alschuler and members of the Jo Daviess County League of Women Voters, especially Elizabeth L. Baranski, for their assistance in locating wells and springs, accessing properties, assisting in sampling, and providing information concerning the presence of karst features throughout Jo Daviess County. The authors thank the Illinois Department of Transportation for acquiring the vertical aerial photography used in this publication. This paper was greatly improved by the reviews and comments of Keith C. Hackley, David R. Larson, Charles W. Knight, Ivan G. Krapac, and Randy Locke of the ISGS, and Jeff Green of the Minnesota Department of Natural Resources. The authors thank Susan Krusemark (editor), Pam Carrillo (graphic artist), and Mike Knapp (graphic artist) of the ISGS for editing the manuscript, drafting figures, and compiling this document.

REFERENCES

American Public Health Association, American Water Works Association, and Water Environment Federation, 1999, Standard methods for the examination of water and wastewater, v. 20: American Public Health Association, American Water Works Association, and Water Environment Federation, https://www.mwa.co.th/download/file_upload/SMWW_1000-3000.pdf (accessed January 30, 2017).

American Society of Photogrammetry and Remote Sensing, 2012, Manual of airborne topographic lidar: Bethesda, Maryland, American Society of Photogrammetry and Remote Sensing, Imaging and Geospatial Information Society.

Bradbury, J.C., 1959, Crevice lead-zinc deposits of northwestern Illinois: Illinois State Geological Survey, Report of Investigation 210, 49 p.

Brannon, J.C., F.A. Podosek, and R.K. McLimans, 1992, Alleghenian age of the Upper Mississippi Valley zinc-lead deposit determined by Rb-Sr dating of sphalerite: Nature, v. 356, p. 509–511.

Ekberg, D.W., 2008, Secondary porosity development in the karstic Galena/Platteville (Trenton/Black River) dolomite on the Wisconsin Arch: Implications for triple porosity ground water flow: National Ground Water Association Ground Water Summit, Memphis, Tennessee, abstract.

Field, M.S., 1993, Karst hydrology and chemical contamination: Journal of Environmental Systems, v. 22, no. 1, 1–26.

Ford, D., and P. Williams, 1989, Karst geomorphology and hydrology: London, Chapman & Hall, 601 p.

Frankie, W.T., 2001, Guide to the geology of the Mississippi Palisades State Park and the Savanna area, Carroll and Jo Daviess Counties, Illinois: Illinois State Geological Survey, Field Trip Guidebook 2001C and 2001D, 78 p.

Frankie, W.T., and R.S. Nelson, 2002, Guide to the geology of the Apple River Canyon State Park and surrounding area of northeastern Jo Daviess County, Illinois: Illinois State Geological Survey, Field Trip Guidebook 2002B, 88 p.

Green, R.T., S.L. Painter, A. Sun, and S.R.H. Worthington, 2006, Groundwater contamination in karst terranes: Water, Air, and Soil Pollution: Focus, v. 6, p. 157–170, doi:10.1007/s11267-005-9004-3.

Haamer, K., and E. Karro, 2006, High fluoride content of K-bentonite beds in Estonia Paleozoic carbonate rocks: Fluoride, v. 39, no. 2, p. 132–137.

Hackley, K.C., S.V. Panno, H.-H. Hwang, and W.R. Kelly, 2007, Groundwater quality of springs and wells in the sinkhole plain in southwestern Illinois: Determination of the dominant sources of nitrate: Illinois State Geological Survey, Circular 570, 39 p.

Hackley, K.C., S.V. Panno, and T. F. Johnson, 2010, Chemical and isotopic indicators of groundwater evolution in the basal sands of a buried bedrock valley in the Midwestern United States: Implications for recharge, rock–water interactions and mixing: Geological Society of America Bulletin, v. 122, p. 1047–1066.

Hansel, A.K., and E.D. McKay III, 2010, Quaternary Period, *in* D.R. Kolata and C.K. Nimz, eds., Geology of Illinois: Illinois State Geological Survey, p. 216–247.

Heyl, A.V., Jr., A.F. Agnew, E.J. Lyons, and C.H. Behre, Jr., 1959, The geology of the upper Mississippi Valley zinc-lead district: U.S. Geological Survey, Professional Paper 309, p. 62–63.

Howard, A.D., 1963, The development of karst features: National Speleological Society Bulletin, v. 25, p. 45–65.

Hwang, H.H., S.V. Panno, and K.C. Hackley, 2015, Sources and changes in groundwater quality with increasing urbanization, northeastern Illinois: Environmental and Engineering Geoscience, v. 21, no. 2, p. p. 75–90.

IDEXX Laboratories, 2013, Colilert: Westbrook Maine, IDEXX Laboratories, Inc., https://www.idexx.com/resource-library/water/colilert-procedure-en.pdf (accessed October 14, 2014).

International Atomic Energy Agency, 2015, WISER: Water isotope system for data analysis, visualization and electronic retrieval: Vienna, Austria, International Atomic Energy Agency, http://www-naweb.iaea.org/napc/ih/IHS_resources_isohis.html (accessed October 14, 2014).

Jennings, J.N., 1971, Karst: Cambridge, Massachusetts, MIT Press, 253 p.

Karst Water Institute (KWI), 2014, What is karst? And why is it important?: Leesburg, Virginia, Karst Water Institute, http://www.karstwaters.org/kwitour/whatiskarst.htm (accessed January 30, 2017).

Kelly, W.R., S.V. Panno, and K.C. Hackley, 2012, Impacts of road salt runoff on water quality of the Chicago, Illinois, region: Environmental and Engineering Geoscience [Special Issue: Hydrogeological Effects of Urbanization], v. 18, no. 1, p. 65–81.

Klimchouk, A.B., and D.C. Ford, 2000, Types of karst and evolution of hydrogeologic setting, *in* A. Klimchouk, D. Ford, A. Palmer, and W. Dreybrodt, eds., Speleogenesis: Evolution of karst aquifers: Huntsville, Alabama, National Speleological Society, p. 45–53.

Kolata, D.R., compiler, 2005, Bedrock geology of Illinois: Illinois State Geological Survey, Illinois Map 14, 1:500,000.

Lindsey, B.D., B.G. Katz, M.P. Berndt, A.F. Ardis, and K.A. Skach, 2010, Relations between sinkhole density and anthropogenic contaminations in selected carbonate aquifers in the eastern United States: Environmental Earth Sciences, v. 60, p. 1073–1090.

Maas, B.J., 2010, Investigation of spatial and temporal variations in water quality around Nora, IL: Bloomington, Illinois State University, master's thesis, 128 p.

Maas, B.J., and E.W. Peterson, 2010, Investigation of spatial and temporal variations in water quality around Nora, IL, *in* Abstracts with Programs: North-Central Geological Society of America 2010, 44th Annual Meeting, paper no. 47-2.

McGarry, C.S., and M.H. Riggs, 2000, Aquifer sensitivity map, Jo Daviess County, Illinois: Illinois State Geological Survey, Open File Series OFS 2000-8i, 1:62,500.

National Centers for Environmental Information, National Oceanic and Atmospheric Administration, 2009, Magnetic declination estimated value: Boulder, Colorado, National Oceanic and Atmospheric Administration, National Centers for Environmental Information, http://www.ngdc.noaa.gov/geomag-web/ (accessed January 30, 2017).

Nelson, J.W., 1995, Structural features in Illinois: Illinois State Geological Survey, Bulletin 100, 144 p.

Nelson, R., and D. Bertalan, directors, 2013, Mysteries of the Driftless: The documentary: Untamed Science, video, 27 min.

O'Riordan, T., and G. Bentham, 1993, The politics of nitrate in the UK, *in* T.P. Burt, A.L. Heathwaite, and S.T. Trudgill, eds., Nitrate—Processes, patterns, and management: New York, John Wiley and Sons, p. 403–416.

Ostlund, H.G., and H.G. Dorsey, 1977, Rapid electrolytic enrichment and hydrogen gas proportional counting of tritium, *in* Low-radioactivity measurements and applications: Proceedings of the International Conference on Low-Radioactivity Measurements and Applications, the High Tatras, Czeckoslovakia: Bratislava, Slovakia, Slovenské Pedagogické Nakladatel'stvo.

Pannalal, S.J., D.T.A. Symons, and D.F. Sangster, 2004, Paleomagnetic dating of Upper Mississippi Valley lead-zinc mineralization, WI, USA: Journal of Applied Geophysics, v. 56, p. 135–153.

Panno, S.V., K.C. Hackley, H.H. Hwang, S. Greenberg, I.G. Krapac, S. Landsberger, and D.J. O'Kelly, 2005, Database for the characterization and identification of the sources of sodium and chloride in natural waters of Illinois: Illinois State Geological Survey, Open File Series 2005-1, 15 p.

Panno, S.V., K.C. Hackley, H.H. Hwang, S. Greenberg, I.G. Krapac, S. Landsberger, and D.J. O'Kelly, 2006a, Characterization and identification of the sources of Na-Cl in ground water: Ground Water, v. 44, no. 2, p. 176–187.

Panno, S.V., K.C. Hackley, H.H. Hwang, and W.R. Kelly, 2001, Determination of the sources of nitrate contamination in karst springs using isotopic and chemical indicators: Chemical Geology, v. 179, no. 1–4, p. 113–128.

Panno, S.V., W.R. Kelly, K.C. Hackley, and C.P. Weibel, 2007, Chemical and bacterial quality of discharge from on-site aeration-type wastewater treatment systems: Ground Water Monitoring Review, v. 27, no. 2, p. 71–76.

Panno, S. V., W. R. Kelly, A.T. Martinsek, and K.C. Hackley, 2006b, Estimating background and threshold nitrate concentrations using probability graphs: Ground Water, v. 44, no. 5, p. 697–709.

Panno, S.V., and D.E. Luman, 2008, Assessment of the geology and hydrogeology of two sites for a proposed large dairy facility in Jo Daviess County near Nora, IL: Illinois State Geological Survey, Open File Series 2008-2, 32 p.

Panno, S.V., D.E. Luman, W.R. Kelly, and M.B. Alschuler, 2013, The use of drought-induced "crop lines" as a tool for characterization of karst terrain, *in* D.H. Doctor and J.B. Stephenson, eds., Proceedings of the 13th Multidisciplinary Conference on Sinkholes and the Engineering and Environmental Impacts of Karst: National Cave and Karst Research Institute Symposium 2, p. 411–419.

Panno, S.V., D.E. Luman, and D.R. Kolata, 2015, Characterization of karst terrain using remotely-sensed data in Jo Daviess County, Illinois: Illinois State Geological Survey, Circular 589, 29 p.; 1 map, 1:62,500; digital appendix at http://isgs.illinois.edu/publications/58/appendix.

Panno, S.V., P.G. Millhouse, R.W. Nyboer, D. Watson, W.R. Kelly, L. Anderson, C.C. Abert, and D.E. Luman, 2014, Guide to the geology, hydrogeology, botany, history and archaeology of the Driftless Area of northwestern Illinois, Jo Daviess County: Illinois State Geological Survey, Field Trip Guidebook 2014A, 70 p.

Panno, S.V., P.G. Millhouse, R.W. Nyboer, D. Watson, W.R. Kelly, L.M. Anderson, C.C. Abert, and D.E. Luman, 2016, Guide to the geology, hydrogeology, history, archaeology, and biotic ecology of the Driftless Area of northwestern Illinois, Jo Daviess County: Illinois State Geological Survey, Guidebook 42, 78 p.

Panno, S.V., and C.P. Weibel, 2010, Karst terrain, *in* D.R. Kolata and C.K. Nimz, Geology of Illinois: Illinois State Geological Survey, p. 432–442.

Panno, S.V., C.P. Weibel, and W.B. Li, 1997, Karst regions of Illinois: Illinois State Geological Survey, Open File Series 1997-2, 42 p.

Panno, S.V., C.P. Weibel, C.M. Wicks, and J.E. Vandike, 1999, Geology, hydrology, and water quality of the karst regions of southwestern Illinois and southeastern Missouri: Illinois State Geological Survey, Guidebook 27, 38 p.

Piskin, K., and R.E. Bergstrom, 1975, Glacial drift in Illinois: Thickness and character: Illinois State Geological Survey, Circular 490, 35 p.

Pluhar, A., and D.C. Ford, 1970, Dolomite karren of the Niagara Escarpment, Ontario, Canada: Zeitschrift für Geomorphologie, v. 14, p. 392–410.

Quinlan, J.F., 1966, A survey on the definition of karst: University of Texas at Astin, unpublished report.

Reed, P.C., 2008, Spring place names and historic data on springs, licks and selected water wells in Illinois: Springfield, Illinois, Capitol Blueprint, 177 p.

Richardson, S.M., and K.S. Hansen, 1991, Stable isotopes in the sulfate evaporites from southeastern Iowa, U.S.A.: Indications of postdepositional change: Chemical Geology, v. 90, p. 79–90.

Riggs, M.H., and C.S. McGarry, 2000, Map showing thickness of Quaternary deposits, Jo Daviess County, Illinois: Illinois State Geological Survey, Open File 2000-8c, 1 sheet.

Rowan, E.L., and G. de Marsily, 2001, Infiltration of Late Paleozoic evaporative brines in the Reelfoot rift: A possible salt source for Illinois basin formation waters and MVT mineralizing fluids: Petroleum Geoscience, v. 7, p. 267–279.

Schilling, K.E., and M. Helmers, 2008a, Effects of subsurface drainage tiles

on streamflow in Iowa agricultural watersheds: Exploratory hydrograph analysis: Hydrological Processes, v. 22, p. 4497–4506, doi:10.1002/hyp.7052.

Schilling, K.E., and M. Helmers, 2008b, Tile drainage as karst: Conduit flow and diffuse flow in a tile-drained watershed: Journal of Hydrology, v. 349, p. 291–301.

Touseull, J., and C. Rich, Jr., 1980, Documentation and analysis of a massive rock failure at the Bautsch Mine, Galena, Illinois: Denver, Colorado, U.S. Department of the Interior, Bureau of Mines, Report of Investigation 8453, 49 p.

Trowbridge, A.C., and E.W. Shaw, 1916, Geology and geography of the Galena and Elizabeth Quadrangles: Illinois State Geological Survey, Bulletin 26, 233 p.

Uppin, M., and E. Karro, 2012, Geological sources of boron and fluoride anomalies in Silurian-Ordovician aquifer system, Estonia: Environmental Earth Science, v. 65, p. 1147–1156.

U.S. Environmental Protection Agency (USEPA), 2014, Sodium in drinking water: Washington, DC, U.S. Environmental Protection Agency, Contaminant Candidate List, http://water.epa.gov/scitech/drinkingwater/dws/ccl/sodium.cfm (accessed January 30, 2017).

Weibel, C.P., and Panno, S.V., 1997, Karst terrains and carbonate bedrock of Illinois: Illinois State Geological Survey, Illinois Map Series 8, 1:500,000.

White, W.B., 1988, Geomorphology and hydrology of karst terrains: New York, Oxford University Press, 464 p.

Willman, H.B., E. Atherton, T.C. Buschbach, C. Collinson, J.C. Frye, M.E. Hopkins, J.A. Lineback, and J.A. Simon, 1975, Handbook of Illinois stratigraphy: Illinois State Geological Survey, Bulletin 95, 261 p.

Willman, H.B., and J.C. Frye, 1970, Pleistocene stratigraphy of Illinois: Illinois State Geological Survey, Bulletin 94, 204 p.